

Exact inference via quasi-conjugacy in two-parameter Poisson–Dirichlet hidden Markov models

MARCO DALLA PRIA

University of Torino

MATTEO RUGGIERO

Stern at NYU Abu Dhabi

DARIO SPANÒ

University of Warwick

December 29, 2025

Abstract

We introduce a nonparametric model for time-evolving, unobserved probability distributions from discrete-time data consisting of unlabelled partitions. The latent process is a two-parameter Poisson–Dirichlet diffusion, and observations arise via exchangeable sampling. Applications include social and genetic data where only aggregate clustering summaries are observed.

To address the intractable likelihood, we develop a tractable inferential framework that avoids label enumeration and direct simulation of the latent state. We exploit a duality between the diffusion and a pure-death process on partitions, together with coagulation operators that encode the effect of new data. These yield closed-form, recursive updates for forward and backward inference.

We compute exact posterior distributions of the latent state at arbitrary times and predictive distributions of future or interpolated partitions. This enables online and offline inference and forecasting with full uncertainty quantification, bypassing MCMC and sequential Monte Carlo. Compared to particle filtering, our method achieves higher accuracy, lower variance, and substantial computational gains. We illustrate the methodology with synthetic experiments and a social network application, recovering interpretable patterns in time-varying heterozygosity.

Keywords: Bayesian nonparametrics; Chinese restaurant process; Filtering and smoothing; Markov duality; Partition structures; Young diagrams.

Contents

1	Introduction	2
2	Partition structures and likelihood representation	4
2.1	Partitions and Ewens–Pitman sampling formula	4
2.2	Likelihood of partition-valued data	5
2.3	Coagulation and likelihood product expansion for partitions	5

3	Filtering two-parameter Poisson–Dirichlet HMMs	7
3.1	Model structure and latent process dynamics	7
3.2	Posterior inference: filtering, smoothing, and forecasting	8
4	Model implementation	14
4.1	Summary of the algorithms	14
4.2	Computability and algorithmic strategies	14
4.3	Parameter estimation	15
4.4	Numerical experiments	16
4.5	Application to dynamic face-to-face interaction networks	18
5	Concluding remarks	19
A	Appendix	20
A.1	Two-parameter Poisson–Dirichlet diffusions	20
A.2	Coagulation of random partitions	21
A.2.1	Two-parameter Poisson–Dirichlet partition structures	21
A.2.2	Coagulation of two-parameter random partitions	21
A.3	A CRP with loss of particles as dual process	23
A.4	Details and proofs on filtering and smoothing	23
A.4.1	Online estimation: filtering and prediction	23
A.4.2	Offline estimation: smoothing and data forecasting	25
A.4.3	Proofs	27
A.5	Implementation	33
A.5.1	Pseudocodes	33
A.5.2	Weights of filtering and smoothing distributions	35
A.5.3	Further figures	36

1 Introduction

We study inference for a latent, continuous-time process of random probability measures observed only through partial summaries. The goal is to recover the law of a time-evolving signal $X(t)$ —an infinite-dimensional vector of decreasing frequencies—from discrete-time observations $Y(t_k)$ given as *unlabelled partitions*.

Such problems arise when the latent structure has unknown or unbounded complexity and only aggregated data are observed. Examples include social networks, where one records sizes of connected components without identities, and biological applications, where species labels are absent and only relative abundances are measured (Bunge and Fitzpatrick, 1993; Holmes et al., 2012; Pritchard et al., 2000). A defining feature is that observations encode frequencies, not labels.

A natural framework is the *hidden Markov model* (HMM), with latent states evolving via a Markov transition and observations conditionally independent given those states (Cappé et al., 2005). Clas-

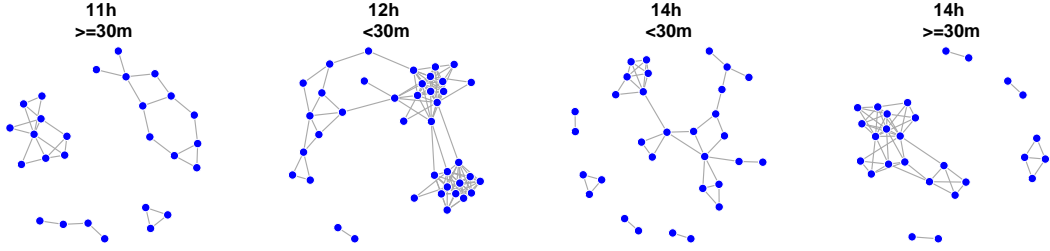


Figure 1: Unlabelled partitions obtained over four intervals from the INFECTIOUS dataset.

sical cases admit exact filters—Kalman, Baum–Welch, Wonham (Kalman, 1960; Baum and Petrie, 1966; Wonham, 1965)—and later work extends to certain diffusions (Chaleyat-Maurel and Genon-Catalot, 2006, 2009; Papaspiliopoulos and Ruggiero, 2014). In more complex settings, inference typically relies on sequential Monte Carlo (SMC) (Chopin and Papaspiliopoulos, 2020).

Here we address a more complex setting: the signal is infinite-dimensional and nonparametric, while observations are combinatorial objects that do not directly index latent components. The inferential goal is to compute filtering distributions $p(x_{t_k} | y_{t_0}, \dots, y_{t_k})$ and related smoothing or predictive laws, which requires structural and computational tools beyond those available for classical HMMs.

Prior work on infinite-dimensional HMMs includes discrete-time models based on Dirichlet and Pitman–Yor processes (Beal et al., 2001; Gael et al., 2008; Chatzis and Tsechpenakis, 2010; Caron et al., 2017) and filters for Fleming–Viot diffusions (Papaspiliopoulos et al., 2016; Ascolani et al., 2023). Here we pursue a continuous-time formulation with latent dynamics given by a two-parameter Poisson–Dirichlet (PD) diffusion (Petrov, 2009; Walker and Ruggiero, 2009; Feng and Sun, 2010). This class, which arises in coalescent theory and population genetics (Costantini et al., 2017; Griffiths et al., 2024), captures power-law clustering but remains largely unexplored in the context of Bayesian nonparametrics.

We therefore propose a new class of infinite-dimensional HMMs where the latent process evolves as a PD diffusion and the observations are unlabelled partitions. These partitions record cluster frequencies without identities (see Section 2.1) and arise naturally in clustering, social networks, and population dynamics.

A motivating example is the INFECTIOUS dataset (Isella et al., 2011), which records time-varying contact networks via wearable sensors. Grouping individuals by connected components yields a sequence of unlabelled partitions, as shown in Figure 1. We revisit this dataset in Section 4.5.

Existing inference methods fail in this regime. SMC requires simulating the diffusion, whose transition law lacks closed form and is costly even when truncated, while MCMC schemes for Dirichlet or Pitman–Yor mixtures rely on labelled structures that are unavailable. Formally, the likelihood of partitions combines an unlabelled likelihood that sums over latent label assignments with an intractable diffusion transition density (see Section 2.2). Both remain computationally prohibitive,

and truncation introduces hard-to-quantify bias, motivating a structural alternative.

We exploit a dual representation of the Poisson–Dirichlet diffusion (Griffiths et al., 2024) as a pure-death process on partitions. This dual evolves backward in time and tracks sufficient statistics of the signal. Combined with new algebraic operations on partitions (*coagulations*), it yields recursive, closed-form updates that enable exact Bayesian inference. In particular, we compute posterior distributions of the latent state at any observation time, smoothing distributions at arbitrary intermediate times, and predictive distributions for future or interpolated partitions, all with full uncertainty quantification.

Our method is a nonparametric analogue of the Baum–Welch filter: in finite-state HMMs, Baum–Welch exploits latent structure to enable exact inference; here we exploit the finite combinatorics of the dual pure-death process to obtain structurally exact filters and smoothers for a continuous-time, infinite-dimensional model. When scalability is needed, the method can be paired with targeted Monte Carlo approximations that preserve the exact update structure while avoiding the inefficiencies of generic SMC or MCMC.

Paper outline. Section 2 develops novel results for partitions and the associated likelihood. Section 3 presents the inferential framework and the main results. Section 4 reports numerical and real-data illustrations, including a comparison with bootstrap particle filtering. Proofs, algorithms, and further details are given in the Appendix.

2 Partition structures and likelihood representation

We collect some key ingredients for inference under the two-parameter Poisson–Dirichlet HMM: (i) the Ewens–Pitman sampling formula, (ii) novel operations on partitions called coagulations, and (iii) a product expansion for the likelihood. These underpin the filtering and smoothing methods of Sections 3–4; full details are in Section A.2.

2.1 Partitions and Ewens–Pitman sampling formula

Let $\pi = (\pi_1, \dots, \pi_{l(\pi)})$ be a partition of n , with non-increasing parts and $\sum \pi_i = n$. The set of such partitions is \mathcal{P}_n , and $\mathcal{P} = \bigcup_{n \geq 1} \mathcal{P}_n$ (Fig. 2, left).

A canonical distribution on partitions is the *Ewens–Pitman sampling formula*:

$$\text{PSF}_{\alpha, \theta}(\pi) := C(\pi) \frac{\prod_{i=0}^{l(\pi)-1} (\theta + i\alpha)}{\theta_{(|\pi|)}} \prod_{j=1}^{l(\pi)} (1 - \alpha)_{(\pi_j - 1)}, \quad (1)$$

with $C(\pi)$ combinatorial (see (17)), $\alpha \in [0, 1)$ and $\theta > -\alpha$. The associated predictive rules correspond to a *Chinese restaurant process* (CRP) with parameters (α, θ) : each new element joins an existing group with probability proportional to the group size (discounted by α), or starts a

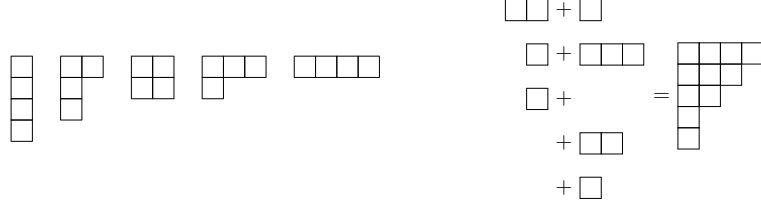


Figure 2: Left: Young diagrams of partitions in \mathcal{P}_4 . Right: indexed coagulation of $\omega = (2, 1, 1)$ and $\gamma = (3, 2, 1, 1)$, yielding $\mu = (4, 3, 2, 1, 1)$.

new group with probability proportional to $\theta + \alpha k$, where k is the current number of groups. See Pitman (2006) for background.

2.2 Likelihood of partition-valued data

Let $\pi^{0:N} = (\pi^0, \dots, \pi^N)$ be observed partitions at $t_0 < \dots < t_N$. The joint likelihood is

$$\Pr(\pi^{0:N}) = \int \dots \int \left[\prod_{k=0}^N P(\pi^k | x_k) p(x_k | x_{k-1}) \right] p(x_0) dx_{0:N}, \quad (2)$$

where $p(x_k | x_{k-1})$ is the transition density of the latent Poisson–Dirichlet diffusion (cf. Sections 3.1 and A.1) and $P(\pi | x)$ the unlabelled likelihood.

For x in the decreasing infinite simplex and $\pi = (\pi_1, \dots, \pi_d)$ a partition of n ,

$$P(\pi | x) = C(\pi) \sum_{i_1 \neq \dots \neq i_d} x_{i_1}^{\pi_1} \cdots x_{i_d}^{\pi_d}, \quad (3)$$

with $C(\pi)$ as in (17). This sums over all latent label assignments consistent with π . Combined with the lack of a closed form for $p(x_k | x_{k-1})$ (see (13) in the Appendix), (2) is analytically intractable, motivating the new methods proposed in Section 3.

2.3 Coagulation and likelihood product expansion for partitions

To enable likelihood-based inference from unlabelled observations, we define operations that merge two partitions. These support posterior updates involving products $P(\omega | x)P(\gamma | x)$ arising in filtering and smoothing.

Definition 1 (Indexed coagulation). *Let $\omega \in \mathcal{P}_m$, $\gamma \in \mathcal{P}_n$. The indexed coagulation of ω and γ assigns parts of γ to subsets of indices in ω , sums assigned entries, and keeps unassigned parts, producing a partition μ coarsening their joint information.*

See Appendix, Def. 3, for a more formal definition. Fig. 2 (right) shows an instance with $\omega = (2, 1, 1)$, $\gamma = (3, 2, 1, 1)$, yielding $\mu = (4, 3, 2, 1, 1)$. The following generalizes Def. 1.

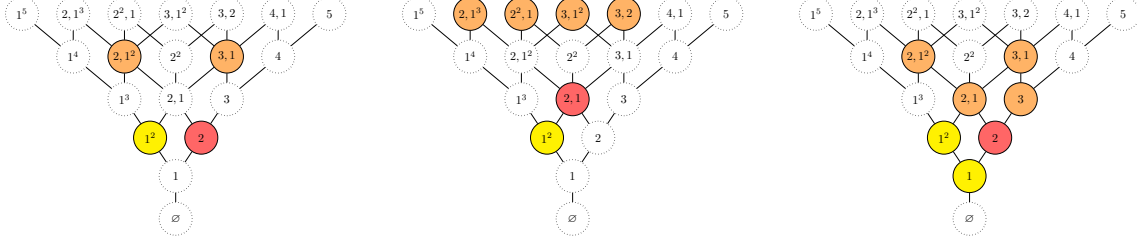


Figure 3: Three examples of coagulation sets $\text{coag}(\Omega, \Gamma)$ (orange) from Ω (yellow) and Γ (red). Left: $\Omega = \{(1, 1)\}$ and $\Gamma = \{(2)\}$ may produce $(2, 1, 1)$ or $(3, 1)$. Right: (2) in Γ merges with (1) or (1^2) , leading to (3) , $(2, 1)$, $(2, 1^2)$, or $(3, 1)$.

Definition 2 (General coagulation). *Let $\omega, \gamma \in \mathcal{P}$. The coagulation set $\text{coag}(\omega, \gamma)$ collects all partitions μ obtainable as indexed coagulations of ω and γ . For sets $\Omega, \Gamma \subset \mathcal{P}$,*

$$\text{coag}(\Omega, \Gamma) := \bigcup_{\omega \in \Omega, \gamma \in \Gamma} \text{coag}(\omega, \gamma).$$

Each $\mu \in \text{coag}(\omega, \gamma)$ arises from a pairing of parts and contributes to posterior support (Fig. 3). In posterior updates, a prior component indexed by ω updated by observation γ yields support $\mu \in \text{coag}(\omega, \gamma)$; this combinatorial framework underlies Section 3.2.

We now state the key product identity for $P(\cdot|x)$ in (3) (proofs in the Appendix).

Proposition 1 (Product expansion). *For any x in the decreasing infinite simplex,*

$$P(\omega|x)P(\gamma|x) = \sum_{\mu \in \text{coag}(\omega, \gamma)} \mathcal{H}(\omega, \gamma|\mu) P(\mu|x),$$

with explicit coefficients $\mathcal{H}(\omega, \gamma|\mu)$ (see Appendix, Proposition 4).

Thus, products of unlabelled likelihoods expand into finite mixtures of the same kernel, evaluated at coagulations. This result provides the foundation for *quasi-conjugacy*: (3) is not closed under multiplication, but admits a finite mixture representation enabling exact Bayesian updates (compare the Binomial likelihood in the Beta–Binomial model).

Proposition 1 is used to characterize predictive distributions under the CRP.

Proposition 2 (Conditional predictive distribution). *Let $\omega \in \mathcal{P}_n$, $\gamma \in \mathcal{P}_m$. Then*

$$\text{CRP}_{\omega \uparrow \gamma} := \Pr(\Pi_{n+1:n+m} = \gamma | \Pi_{1:n} = \omega) = \sum_{\mu \in \text{coag}(\omega, \gamma)} \mathcal{H}(\omega, \gamma|\mu) \frac{\text{PSF}_{\alpha, \theta}(\mu)}{\text{PSF}_{\alpha, \theta}(\omega)}. \quad (4)$$

When $\omega = \emptyset$, this reduces to (1).

This yields exact, closed-form predictive laws under the Ewens–Pitman model of Sec. 2.1, expressed as finite mixtures indexed by coagulated partitions. Related distributions used in filtering and smoothing are discussed in the SM. In Section A.3, we discuss how a dual pure-death process (Griffiths et al., 2024) aligns with these structures. We leverage this duality in Section 3 to enable recursive exact filtering and smoothing.

3 Filtering two-parameter Poisson–Dirichlet HMMs

3.1 Model structure and latent process dynamics

We now formalize the statistical model. The latent process is a two-parameter Poisson–Dirichlet diffusion $X := (X(t), t \geq 0)$, with parameters (α, θ) for $0 \leq \alpha < 1$ and $\theta \geq -\alpha$. This infinite-dimensional process models time-evolving frequencies of unobserved categories—e.g., species proportions or cluster sizes in graphs (cf. Fig. 1)—with continuous paths in the ordered infinite simplex, i.e., decreasingly ordered vectors summing to 1. We assume $X(0) \sim \text{PD}_{\alpha, \theta}$, the stationary law. See Section A.1 for background.

At discrete times $t_0 < t_1 < \dots < t_N$, we observe unlabelled partitions $\Pi^k \in \mathcal{P}_{n_k}$ formed by drawing n_k samples from $X(t_k)$ and grouping them by type, encoding block sizes without tracking labels (Fig. 2, left). The model follows a hidden Markov structure:

$$X(t_k) \sim \text{PD}_{\alpha, \theta}, \quad \Pi^k | X(t_k) \sim \text{Part}(n_k, X(t_k)). \quad (5)$$

Here the observations Π^k are independent, conditional on $X(t_k)$, and the distribution $\text{Part}(n, x)$ corresponds to Kingman’s *paintbox construction*. Specifically, samples are independently assigned to indices $i \in \mathbb{N}$ with probabilities x_i , and grouped by common index, and the resulting unlabelled partition records only block sizes. Crucially, all permutations of labels that yield the same block structure are treated as equivalent, as the partition is invariant under relabelling.

Marginalizing over $X(t_k)$ yields that Π^k has law (1). This defines a nonparametric HMM with infinite-dimensional hidden states and discrete, combinatorial observations.

Next, we describe the latent signal dynamics, and discuss their intractability.

Latent dynamics. The conditional law of $X(t_k)$ given $X(t_{k-1})$ can be described through a latent partition induced by sampling from $X(t_{k-1})$. This yields the generative hierarchy:

$$\begin{aligned} N_k &\sim \mathcal{B}_\theta(\Delta_k), \quad \Delta_k := t_k - t_{k-1}, \\ \lambda(t_k) | N_k = n, X(t_{k-1}) = x &\sim \text{Part}(n, x), \\ X(t_k) | \lambda(t_k) = \lambda &\sim \text{PD}_{\alpha, \theta}^\lambda. \end{aligned} \quad (6)$$

Interpretation is as follows. An integer N_k is drawn from $\mathcal{B}_\theta(\Delta_k)$, the distribution of the number of *blocks* in Kingman’s coalescent, a pure-death process which starts from infinity (Section A.1). Conditional on $N_k = n$, n latent samples are drawn from $X(t_{k-1})$ to induce the latent partition $\lambda(t_k) \sim \text{Part}(n, x)$ (cf. (5)). Finally, $X(t_k)$ is updated via the posterior $\text{PD}_{\alpha, \theta}^\lambda$ (to be described shortly). Note that N_k depends on Δ_k but not on x , and governs temporal dependence: small Δ_k yields large N_k and strong dependence, with $\Delta_k \rightarrow 0$ recovering continuity, while large Δ_k induces near-independence, $\Delta_k \rightarrow \infty$ leading to stationarity ($X(t_k) \sim \text{PD}_{\alpha, \theta}$). See Section A.1 for details.

The posterior law $\text{PD}_{\alpha,\theta}^\lambda$ was characterized by Pitman (2006) in the *labelled* case; see Griffiths et al. (2024, Prop. 4.1) for the *unlabelled* case. Let $\text{Dir}(\beta_1, \dots, \beta_m)$ be a Dirichlet distribution and Π a generic random partition. If $X \sim \text{PD}_{\alpha,\theta}$ and $\Pi|X \sim \text{Part}(n, X)$, then

$$(X|\Pi = \pi) \stackrel{d}{=} ((1-W)X_1^{(1)}, \dots, (1-W)X_{l(\pi)}^{(1)}, WX_1^{(2)}, WX_2^{(2)}, \dots)^\downarrow, \quad (7)$$

where $(\cdot)^\downarrow$ denotes decreasing rearrangement, and the components are independent:

$$W \sim \text{Beta}(\theta + \alpha l(\pi), n - \alpha l(\pi)), \quad X^{(1)} \sim \text{Dir}(\pi_1 - \alpha, \dots, \pi_{l(\pi)} - \alpha), \quad X^{(2)} \sim \text{PD}_{\alpha, \theta + \alpha l(\pi)}.$$

Although not a $\text{PD}_{\alpha,\theta}$, we denote the law of $X|\Pi = \pi$ in (7) by $\text{PD}_{\alpha,\theta}^\pi$ for notational convenience.

Remark 1. *A singleton makes an exception, since $\text{PD}_{\alpha,\theta}^{(1)} \stackrel{d}{=} \text{PD}_{\alpha,\theta}$; this is peculiar to unlabelled models, since an observed singleton carries no information on the grouping structure.*

Sampling from $\text{PD}_{\alpha,\theta}^\pi$ is feasible via Algorithm 2, which relies on ε -truncated simulation methods (Algorithm 1). See Section A.5.

In the next section we show that the HMM (5) also admits a conditional independence representation given a latent partition. This parallels (6), but crucially involves only finite computations.

Notation for conditional laws. We let $\nu_{k|h:j}(A) := \Pr_{\alpha,\theta}(X(t_k) \in A | \Pi^h, \dots, \Pi^j)$ denote the law of $X(t_k)$ given observations in $[t_h, t_j]$. This accommodates: filtering: $k = j$ (online estimation); prediction: $k > j$ (forecasting); smoothing: $k < j$ (offline estimation).

3.2 Posterior inference: filtering, smoothing, and forecasting

Direct use of the transition dynamics (6) is intractable. We instead exploit a *dual* representation of the PD diffusion in terms of a pure-death process $N(t)$ with finite starting point (Griffiths et al., 2024). This duality allows the transition $X(t_k) | X(t_{k-1})$ to be expressed, conditionally on observed data, through a latent partition with finite support, yielding tractable recursive filtering.

We now summarize the main inferential results for the two-parameter Poisson–Dirichlet HMM (5), with full details in the Appendix (Sections A.4.1–A.4.2).

General posterior representation. All posterior laws of interest—including filtered, smoothed, and interpolated distributions—belong to the following finite mixture family:

$$\mathcal{F} := \left\{ \nu = \sum_{\lambda \in \Lambda} w_\lambda \text{PD}_{\alpha,\theta}^\lambda : \Lambda \subset \mathcal{P}, |\Lambda| < \infty, \sum w_\lambda = 1 \right\}, \quad (8)$$

with each $\text{PD}_{\alpha,\theta}^\lambda$ as in (7) and weights w_λ being explicit functions of the observations.

The key structural feature is that \mathcal{F} is closed under prediction and update, yielding recursive filtering and smoothing procedures. Thus, despite the infinite-dimensional nature of the signal, all posterior distributions for $X(t)$ evolve within a finite-dimensional, tractable space. Model (5) is thus *quasi-conjugate*, in the sense that at any t , unconditionally we have $X(t) \sim \text{PD}_{\alpha,\theta}$, while given observed data

$$X(t)|\Pi^{0:N} \sim \sum_{\lambda \in \Lambda_t} w_\lambda(t) \text{PD}_{\alpha,\theta}^\lambda, \quad (9)$$

with $\Lambda_t \subset \mathcal{P}$ being a finite and deterministic set determined by the data. This quasi-conjugacy mirrors the role of conjugate priors in parametric models: although the likelihood is not closed under multiplication, Proposition 1 shows that products of likelihoods decompose as finite mixtures of the same kernel, preserving tractability.

Equivalently, (9) corresponds to the hierarchy

$$X(t)|\lambda(t) = \lambda \sim \text{PD}_{\alpha,\theta}^\lambda, \quad \lambda(t)|\Pi^{0:N} \sim w_\bullet(t),$$

where w_λ has finite support and reflects the full observation history. The evolution of these latent quantities (sets Λ_t and weights $w_\lambda(t)$) is governed explicitly by the dual process and the coagulation algebra introduced in Section 2.3.

Online estimation (filtering). We compute the filtered distribution of the latent state at observation time t_k as a finite mixture

$$\nu_{k|0:k} = \Pr(X(t_k) \in \cdot | \Pi^{0:k}) = \sum_{\lambda \in \Lambda_{0:k}} w_\lambda \text{PD}_{\alpha,\theta}^\lambda,$$

where $\Lambda_{0:k} \subset \mathcal{P}$ is a finite collection of partitions determined by the data collected up to time t_k , and w_λ are explicitly computable data-dependent weights (we will drop the dependence of $w_\lambda(t)$ on t for notational convenience when this causes no confusion). The posterior retains the structure of a finite mixture of conditionally conjugate components $\text{PD}_{\alpha,\theta}^\lambda$, which is preserved under recursive prediction and update operations. Define the *lower set* of $\Lambda \subset \mathcal{P}$ to be

$$L(\Lambda) = \{\omega : \omega \preccurlyeq \lambda, \lambda \in \Lambda\},$$

i.e., the set of partitions that can be obtained by removing objects from partitions in Λ .

Proposition 3 (Recursive filtering structure). *Let the latent state $X(t_{k-1})$ conditional on the partitions $\Pi^{0:k-1}$ observed up to time t_{k-1} have posterior distribution $\nu_{k-1|0:k-1} = \sum_{\lambda \in \Lambda} w_\lambda \text{PD}_{\alpha,\theta}^\lambda$. Then, at time t_k :*

(i) **Prediction.** *The law $\nu_{k|0:k-1}$ of the latent state $X(t_k)$ conditional on the partitions $\Pi^{0:k-1}$ observed up to time t_{k-1} belongs to \mathcal{F} . In particular,*

$$X(t_k)|\lambda(t_k) \sim \text{PD}_{\alpha,\theta}^{\lambda(t_k)}, \quad \lambda(t_k) \sim \sum_{\lambda \in \Lambda} w_\lambda p_{\lambda,\bullet}^\downarrow(\Delta_k), \quad (10)$$

where $p_{\lambda, \bullet}^{\downarrow}(\Delta_k)$ are the transition probabilities of the dual (cf. (21)).

(ii) **Update.** Let $v_\omega := \Pr(\lambda(t_k) = \omega)$ denote the distribution of $\lambda(t_k)$ in (10), and let $\Pi^k = \pi^k$ be the observed partition at time t_k . Then the law $\nu_{k|0:k}$ of the latent state $X(t_k)$ conditional on the partitions $\Pi^{0:k}$ observed up to time t_k belongs to \mathcal{F} . In particular,

$$X(t_k)|\lambda(t_k) \sim \text{PD}_{\alpha, \theta}^{\lambda(t_k)}, \quad \lambda(t_k)|\pi^k \sim \sum_{\omega \in L(\Lambda)} \hat{v}_\omega \text{Coag}_{\alpha, \theta}(\omega, \pi^k), \quad (11)$$

where $\hat{v}_\omega \propto v_\omega \text{CRP}_{\omega \uparrow \pi^k}$, $\text{CRP}_{\omega \uparrow \pi^k}$ is as in (4), and $\text{Coag}_{\alpha, \theta}(\omega, \pi^k)$ is fully described in (19).

This result highlights the key structural property of the filtering scheme: the latent state $X(t_k)$, conditioned on data $\Pi^{0:k}$, always admits a finite mixture representation over posterior distributions $\text{PD}_{\alpha, \theta}^{\lambda}$. See Theorems 2 and 3 for alternative formulations equivalent to (10) and (25).

The recursive construction unfolds over two alternating stages, each preserving membership in the mixture family \mathcal{F} :

- The *prediction step* (part (i)) advances the prior distribution from t_{k-1} to t_k via the dual block-counting process. This process propagates the latent partition $\lambda(t_{k-1})$ forward in time, producing a new latent partition $\lambda(t_k)$ according to the death process transitions $p_{\lambda, \bullet}^{\downarrow}(\Delta_k)$. Conditionally on $\lambda(t_k)$, the state $X(t_k)$ is distributed as $\text{PD}_{\alpha, \theta}^{\lambda(t_k)}$, preserving analytic tractability.
- The *update step* (part (ii)) incorporates the new observation $\Pi^k = \pi^k$ by modifying the law of the latent partition $\lambda(t_k)$ through the coagulation operation. Each predicted partition is merged with the observed data to produce an updated pool of information. Again, conditionally on $\lambda(t_k)$, the law of $X(t_k)$ remains in the conjugate class $\text{PD}_{\alpha, \theta}^{\lambda(t_k)}$.

In both steps, the latent partition $\lambda(t_k)$ plays a central role: it acts as a sufficient statistic for the posterior component, while its evolution is governed by the dual process (for prediction) and by the algebra of coagulations (for updates). Crucially, the distribution of the latent partition summarizes the relevant information accrued up to time t_k . Hence, filtering in the two-parameter Poisson–Dirichlet model can be interpreted as tracking the evolution of this latent partition, rather than the infinite-dimensional law of $X(t)$ directly.

Moreover, the recursion is closed in the sense that it only involves a finite and tractable number of latent partitions at each time step. The support Λ_t of the mixture evolves deterministically, and the updated weights can be computed explicitly. This renders the inference scheme fully analytic and computationally efficient, with no need for Monte Carlo methods.

In summary, the recursive filtering algorithm maintains tractability by leveraging the dual structure of the PD diffusion and the partition algebra. The hidden state $X(t_k)$ is always conditionally

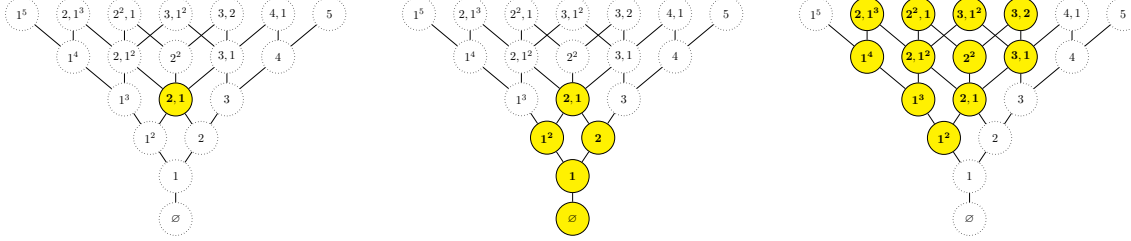


Figure 4: Latent partition support in recursive filtering via prediction and update. Left: initial support $\Lambda = \{(2, 1)\}$ at t_0 . Center: prediction expands Λ this to $L(\Lambda)$ using the dual process. Right: update with $\pi^1 = (1, 1)$ produces $\text{coag}(L(\Lambda), \pi^1)$ as the new support. Each node represents a component $\text{PD}_{\alpha, \theta}^\lambda$.

distributed as a finite mixture of $\text{PD}_{\alpha, \theta}^\lambda$ distributions, where each λ reflects a possible state of a latent, unobserved partition $\lambda(t_k)$ guided by past data and current observations.

Fig. 4 illustrates this process: an initial observed partition $\pi^0 = (2, 1)$ (left graph) yields posterior $X(t_0) \sim \text{PD}_{\alpha, \theta}^{(2, 1)}$. The prediction step computes a lower set $L((2, 1))$ via the dual death process (center graph), forming the support of the latent partitions in $\nu_{1|0}$. Then, observing $\pi^1 = (1, 1)$ leads to the updated support $\text{coag}(L((2, 1)), (1, 1))$ (right graph) through the product expansion. The recursion continues analogously at later times.

This structure enables fast and tractable online inference: filtering requires only propagation and update of a finite set of partitions λ and their weights w_λ , with no need for simulation or numerical integration.

Offline estimation (smoothing). While filtering tracks the evolving law of the latent state $X(t_k)$ using data up to time t_k , smoothing provides retrospective estimates by conditioning on the full observation sequence $\Pi^{0:N}$. The goal is to compute the distribution of $X(t_k)$ given all data, i.e., $\nu_{k|0:N} = \Pr(X(t_k) \in \cdot | \Pi^{0:N})$, for arbitrary $0 \leq k \leq N$.

The key insight is that smoothing retains the same latent partition structure as filtering: at any time t_k , the smoothed distribution of $X(t_k)$ remains a finite mixture over conditionally conjugate components $\text{PD}_{\alpha, \theta}^\mu$, where each index μ reflects a plausible state of the latent partition consistent with both past and future data. As in filtering, the latent partition act as sufficient statistics for posterior inference, and their evolution is governed by algebraic operations on partitions.

Smoothing is achieved by combining: (i) the forward information from the filter at time t_k , encoded by a finite collection $\Lambda_{0:k}$ of partitions and their associated weights; and (ii) future information propagated backwards from time t_N up to t_k , encoded by a finite support $\Omega^{k:N}$ of partitions that are compatible with future data.

At a high level, the smoothing algorithm proceeds as follows:

- Run the forward filtering recursion up to time t_k to obtain $\Lambda_{0:k}$
- Run a backward pass from t_N down to t_{k+1} , and propagate further to t_k , constructing a

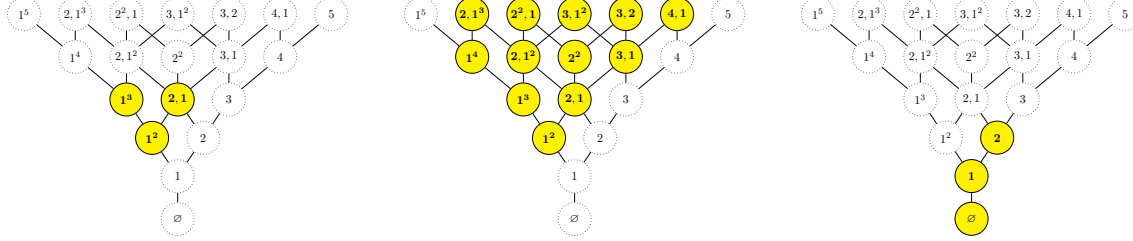


Figure 5: Smoothing via forward-backward latent structure. The *forward* latent partition support $\Lambda_{0:k}$ (left) is coagulated with the *backward* latent partition support $\Omega^{k:N}$ (right), to form the coagulation set $\text{coag}(\Lambda_{0:k}, \Omega^{k:N})$ (middle). The latter supports the latent partitions in the posterior law of $X(t_k) | \Pi^{0:N}$.

compatible set of backward partitions $\Omega^{k:N}$.

- For each pair $(\lambda, \omega) \in \Lambda_{0:k} \times \Omega^{k:N}$, form a new set of partitions $\text{coag}(\lambda, \omega)$.
- Assign to each coagulation μ thus obtained, hence to $\text{PD}_{\alpha, \theta}^\mu$, a weight computed from the product of the forward and backward contributions.

The resulting posterior distribution is a finite mixture over partitions μ , each representing a coherent reconstruction of the system state at time t_k consistent with the full dataset.

Despite the bidirectional nature of the algorithm, tractability is fully preserved. All steps involve only finite sets of partitions, and weights can be computed exactly using closed-form expressions. No simulation or numerical integration is required. Full mathematical details, including the mixture representation and formal proof of correctness, are provided in Theorem 4 of the Appendix.

Forecasting and interpolation. The same recursive structure extends naturally to inference at unobserved time points. For forecasting beyond the last observation time t_N , the distribution of the latent state $X(t)$ for $t > t_N$ is obtained by propagating the filtered distribution $\nu_{N|0:N}$. Thanks to Theorem 2 in the Appendix, this again takes the form (9), where the weights $w_\lambda(t)$ reflect the evolution of the dual process beyond the observation window. E.g., if at t_N the latent partition has support as in the rightmost graph of Fig. 4, call it $\Lambda_{0:N}$, then Λ_t in (9) is the lower set $L(\Lambda_{0:N})$, which in this case is the union of $\Lambda_{0:N}$ with $\{(3), (2), (1), \emptyset\}$. As the forecast horizon grows ($t \rightarrow \infty$), the probability mass over $L(\Lambda_{0:N})$ progressively concentrates towards node in a neighborhood of \emptyset , implying that influence of past data vanishes and the forecast distribution converges to the stationary law $\text{PD}_{\alpha, \theta}$ (cf. Corollary 1).

Finally, if one seeks to interpolate between observation times to estimate $X(t)$ for $t \in (t_k, t_{k+1})$, the posterior takes again a qualitatively similar form, but the weights depend explicitly on the time offset $t - t_k$. This is formalized in Corollary 2, enabling smoothed inference at arbitrary intermediate time points.

Predictive functionals. A byproduct of the above results is that the law of future or interpolated data $\Pi'(t)$ induced by m samples from $X(t)$ is a finite mixture of predictive CRP distributions. Specifically

$$\Pi'(t)|\lambda(t) = \lambda \sim \text{CRP}_{\lambda \uparrow \bullet}, \quad \lambda(t)|\Pi^{0:N} \sim w_\bullet(t)$$

with $\text{CRP}_{\lambda \uparrow \bullet}$ as in (4). In particular, if $t > t_N$, this is achieved by evolving the current sufficient statistic $\lambda(t_N)$ forward in time through the dual process to obtain $\{w_\lambda(t), \lambda \in \Lambda_t\}$. Then, conditional on $\lambda(t) = \lambda$, a future observation $\Pi'(t)$ has law $\text{CRP}_{\lambda \uparrow \bullet}$. This yields interpretable predictions and simulations of future observations.

More generally, our framework enables exact posterior predictive inference for functionals of the latent measure $X(t)$, such as entropy or heterozygosity, i.e., the probability that two randomly chosen individuals belong to different types. This is obtained by applying explicit moment formulas for $\text{PD}_{\alpha,\theta}$ laws. For instance, heterozygosity corresponds to the second moment of $X(t)$, which admits a closed-form expression. This allows principled forecasting and uncertainty quantification for summary statistics of interest, without requiring forward simulation or numerical integration.

We summarize the above results in the following theorem.

Theorem 1 (Exact inference for PD-HMMs). *Let $X = (X(t), t \geq 0)$ be a $\text{PD}_{\alpha,\theta}$ -diffusion observed via partition-valued data Π^0, \dots, Π^N as in (5), and let \mathcal{F} be as in (8). Then:*

1. **Filtering and prediction.** For each $k \leq N$ and $h \geq 0$, the filtering and forecast distributions $\nu_{k|0:k}$ and $\nu_{k+h|0:k}$ belong to the family \mathcal{F} , and are computable via a recursive procedure based on finite-lattice transitions (cf. Theorems 2–3).
2. **Smoothing.** For each $k < N$, the smoothed distribution $\nu_{k|0:N}$ also lies in \mathcal{F} and is obtained through a backward-forward recursion over partitions (cf. Theorem 4).
3. **Forecasting new data.** For any $t \in [0, \infty)$ and $n \in \mathbb{N}$, the conditional distribution of a new data point $\Pi'(t)$ given $\Pi^{0:N}$ is a finite mixture of conditional CRP distributions (cf. Corollary 3).

All mixture components and weights in Theorem 1 are available in closed form and detailed in the Appendix, as well as algorithms for exact simulation and evaluation (cf. Algorithms 3–8).

Theorem 1 establishes that posterior inference for the hidden model (5) is tractable: all relevant conditional distributions admit closed-form expressions as finite mixtures of quasi-conjugate components, with no need for Markov chain Monte Carlo or Sequential Monte Carlo approximations. This result enables exact recursive inference for infinite-dimensional nonparametric latent dynamics, using only combinatorial structures on partitions. Fig. 6 illustrates the resulting inferential procedures, which unify prediction, filtering, smoothing, and interpolation within a single coherent framework.

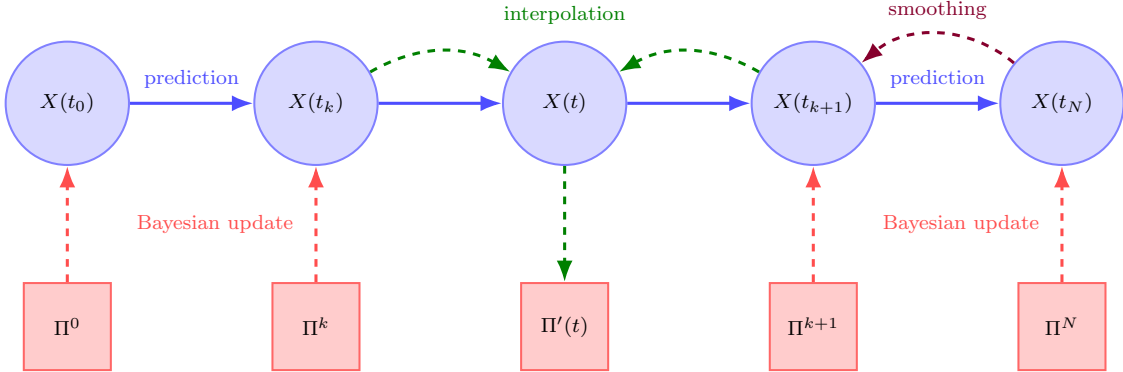


Figure 6: Recursive inference in the hidden PD model. Arrows denote prediction (solid blue), Bayesian update (dashed red), interpolation (dashed green), and backward smoothing (dashed purple).

4 Model implementation

4.1 Summary of the algorithms

The full filtering and smoothing procedures, including intermediate computational steps, are detailed in the pseudocodes provided in Section A.5. In particular, Algorithms 1 and 2 serve as auxiliary routines for simulating from an ε -truncated $\text{PD}_{\alpha,\theta}$ distribution and a conditional ε -truncated $\text{PD}_{\alpha,\theta}^\pi$, respectively. The core inferential operations are handled by the remaining algorithms: Algorithm 3 samples from the propagation step (cf. (10)); Algorithm 5 covers the update step (cf. (25)); and Algorithm 6 combines these components to perform online filtering via the recursive operations (cf. (23)). For offline inference, Algorithms 7 and 8 support latent state estimation and partition simulation, respectively, after observing the full dataset.

4.2 Computability and algorithmic strategies

When initialized at $X(0) \sim \text{PD}_{\alpha,\theta}$, the latent system satisfies *computability* in the sense of Chaleyat-Maurel and Genon-Catalot (2006): all conditional distributions of $X(t)$ lie in the finite mixture family \mathcal{F} of Equation (8), and thus admit exact evaluation without resorting to stochastic truncation, MCMC, or SMC.

Nevertheless, efficient approximations are often desirable. Two key aspects are addressed in our implementation. First, computing the mixture weights $p_{\lambda,\bullet}^\downarrow(t)$ in Equation (24)—the transition probabilities of a pure-death process on \mathcal{P} —can be computationally intensive. Although exact formulas are available, we use a Monte Carlo approach based on the Gillespie algorithm (Gillespie, 2007) to simulate paths of the death process (see Algorithm 4). This approximation may encounter numerical difficulties when starting from large partitions and propagating over short time intervals; in such cases, Gaussian approximations (Griffiths, 1984) provide a useful alternative.

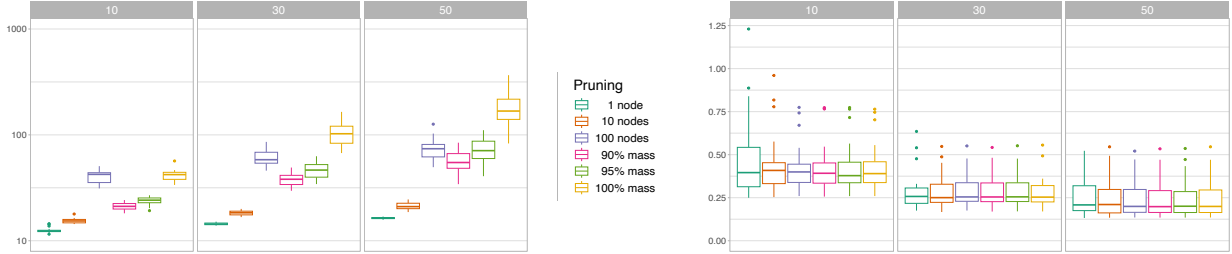


Figure 7: Left: Runtime (seconds, log scale) of Algorithm 6 for sample sizes $|\gamma| = 10, 30, 50$, and various pruning strategies (top-weighted components or total mass thresholds). Filtering draws 10^4 samples after each update using Algorithm 4. Parameters: $\alpha = 0.1$, $\theta = 1.5$, $N = 9$, $\Delta_k = 0.2$ for all k , with $\text{PD}_{\alpha, \theta}$ truncation threshold $\varepsilon = 0.005$. Right: Associated negatively oriented interval scores (Equation (12)) based on 95% credible intervals for heterozygosity.

The second computational challenge arises from the rapid growth of the partition space as sample size increases. However, even in the unlabelled setting, most of the mixture’s probability mass is typically concentrated on a small subset of components. Fig. 11 illustrates this concentration, showing that mixtures pruned to include only components with cumulative weight above a chosen threshold (e.g., 95%) retain most of the mass. Accordingly, we adopt pruning techniques as in Kon Kam King et al. (2021, 2024), either by retaining components up to a fixed cumulative mass or selecting the top components by weight.

As shown in Fig. 7, substantial speed gains result from pruning, especially at larger sample sizes. Pruning to 90% total mass or retaining 10 components delivers near-identical accuracy compared to using the full mixture. The accuracy here is quantified by the *negatively-oriented interval scores* (Gneiting and Raftery, 2007)

$$\mathcal{S}^{(N)} = \frac{1}{N} \sum_{k=0}^N \mathcal{S}_\kappa(l_{t_k}, u_{t_k}, y_{t_k}), \quad (12)$$

where $\mathcal{S}_\kappa(l, u, y) = (u - l) + \frac{2}{\kappa}(l - y)\mathbb{1}\{y < l\} + \frac{2}{\kappa}(y - u)\mathbb{1}\{y > u\}$, and l, u are the $\kappa/2$ and $1 - \kappa/2$ quantiles of the filtering distribution for a functional quantity y . This score measures forecast accuracy by penalizing both the width of the predictive interval and any observations that fall outside it, with lower values indicating better performance. We apply this to the heterozygosity $H_2(x) := 1 - \sum_{j \geq 1} x_j^2$, comparing its true value with the 95% credible intervals from the filter. Our results support pruning as a valid and efficient approach for practical implementation.

4.3 Parameter estimation

Joint inference for (α, θ) in the $\text{PD}_{\alpha, \theta}$ model is nontrivial, even in static or labelled settings (see Balocchi et al., 2022; Cereda et al., 2023). In our dynamic unlabelled setting, we estimate these parameters via maximum likelihood using the sequence of filtering distributions, thereby directly targeting the evolving latent trajectory.

The marginal likelihood of the observed data sequence is given by

$$\Pr(\Pi^0 = \pi^0, \dots, \Pi^N = \pi^N) = \text{PSF}_{\alpha, \theta}(\pi^0) \prod_{k=1}^N \sum_{\omega \in L(\Lambda_{0:k-1})} v_\omega \text{CRP}_{\omega \uparrow \pi^k}$$

where the weights v_ω are those of the propagated law of the latent partition as given in Proposition 3; cf. (1) and (4). Each term on the right-hand side corresponds to a predictive partition distribution, which can be computed from Corollary 3 and is readily available from the weights computed during the update step in Algorithm 5. Thus, maximum likelihood can be implemented as a by-product of online inference.

4.4 Numerical experiments

We illustrate our methodology using synthetic data from a known $\text{PD}_{\alpha, \theta}$ diffusion trajectory. The goal is to estimate the heterozygosity functional of the latent state x , given by $H_2(x) := 1 - \sum_{j \geq 1} x_j^2$. Although we focus on H_2 , our approach can be readily adapted to other functionals on the ordered infinite simplex, such as entropy and concentration indices (Patil and Taillie, 1982).

A latent trajectory is simulated at 10 equispaced time points ($\Delta_k = 0.025$) with $(\alpha, \theta) = (0.1, 1.5)$, and observations are generated as unlabelled partitions of size 50 from model (5). Filtering and smoothing are performed via Algorithms 6 and 7, using pruning to retain the 10 mixture components with largest weights after each propagation and update step. Gillespie-based propagation uses 10^4 particles (Algorithm 4), and posterior summaries are computed from 10^4 posterior draws.

Model parameters are estimated by maximizing the marginal likelihood over a discrete grid, yielding $(\hat{\alpha}, \hat{\theta}) = (0, 1.5)$ —slightly underestimating α . Fig. 8 displays marginal posterior estimates for $H_2(x)$ at the observed time points. Violin plots represent posterior densities (via kernel density estimation), triangles mark 95% credible intervals, and white diamonds indicate the observed heterozygosities $\hat{H}_2(\pi^k) = 1 - \sum_j (\pi_j^k / |\pi^k|)^2$. Both the filtering and smoothing procedures (top panels) successfully track the true heterozygosity trajectory (black line), even under this slight model mismatch. See Section A.5.3 for further plots.

Notably, our duality-based filter achieves superior accuracy compared to the Bootstrap Particle Filter (BPF)—a leading benchmark in the literature (Chopin and Papaspiliopoulos, 2020). While the BPF (bottom left panel) performs reasonably well, it requires expensive simulation of $\text{PD}_{\alpha, \theta}$ -diffusion paths (Eq. (6)) and exact importance weight computations (Eq. (3)) for each particle and time step, leading to substantial computational overhead. Furthermore, as seen in Fig. 8, the BPF may occasionally yield posteriors with greater variance and pronounced multimodality, especially at intermediate time points (cf. also Section 4.5).

By contrast, our duality-based approach avoids such burdens, yielding stable, high-quality estimates at a fraction of the computational cost.

Finally, as shown in the bottom right panel, inference based on independent priors—that is, ignoring

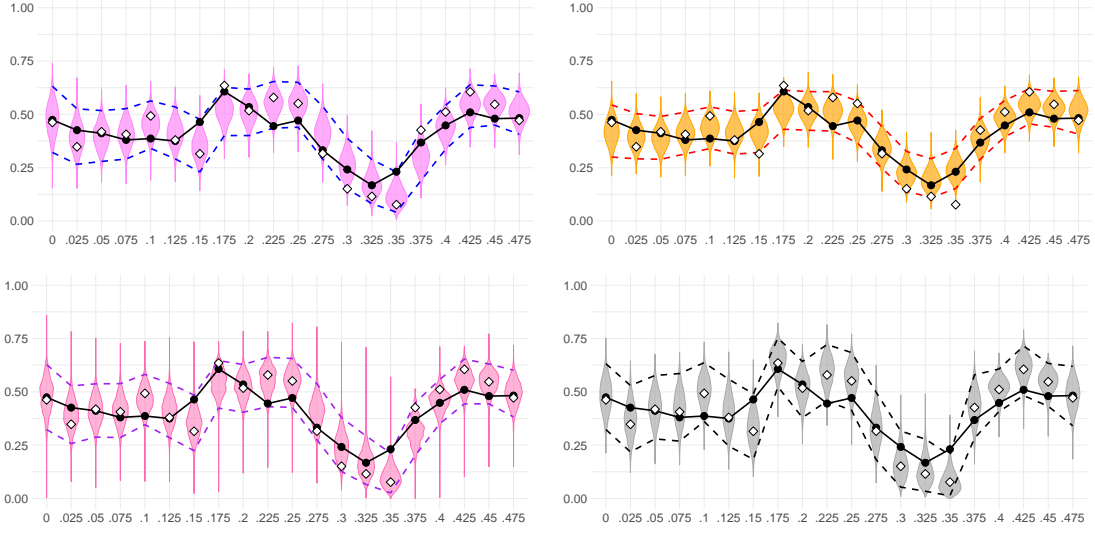


Figure 8: Posterior inference for heterozygosity using filtering (top left), smoothing (top right), bootstrap particle filter (bottom left) and independent priors (bottom right). Black line: true H_2 trajectory; white diamonds: observed heterozygosity $\hat{H}_2(\pi^k)$. Violin plots show posterior densities; dashed lines show 95% credible intervals.

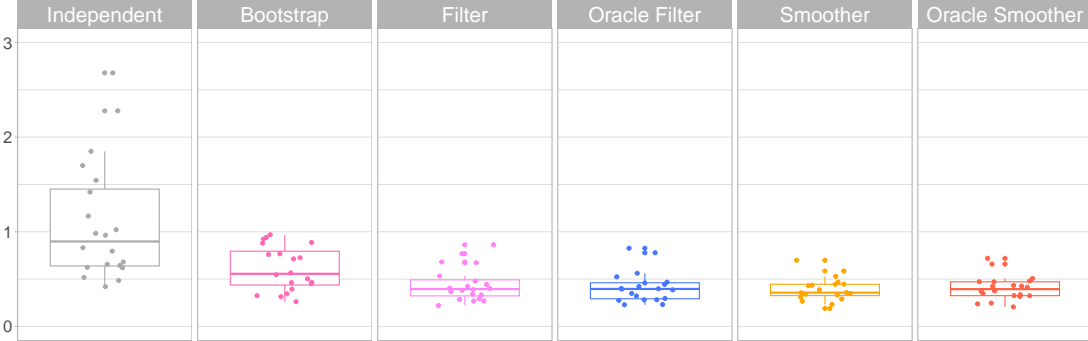


Figure 9: Interval score comparison across five methods. Filtering and smoothing based on MLEs perform comparably to oracle methods. Bootstrap particle filtering yields less accurate results besides being more demanding computationally. Independent priors yield lower accuracy due to lack of temporal borrowing.

temporal dependence—may incidentally approximate the true heterozygosity but lacks robustness and statistical adequacy in dynamic or data-sparse regimes. It also precludes interpolation at arbitrary time points, which our model handles naturally and with no additional effort.

To assess accuracy, we compare negatively-oriented interval scores (cf. (12)) across six strategies: (i) independent priors at each time point, (ii) bootstrap particle filtering, (iii) filtering with MLE parameters, (iv) *oracle* filtering using true parameters, (v) smoothing with MLE parameters, and (vi) *oracle* smoothing using true parameters.

Fig. 9 reports the average scores over 20 replicates of trajectories, each spanning 10 time points with $\Delta_k = 0.01$, partition size 10, and parameters $(\alpha, \theta) = (0.1, 1.0)$. Our filtering and smoothing methods significantly outperform the independent prior baseline and approach the accuracy of an oracle with full knowledge of the latent process. The BPF improves over the independent prior baseline but still falls short of both filtering and smoothing under our duality-based framework, and does so at a substantially higher computational cost.

4.5 Application to dynamic face-to-face interaction networks

We apply our methodology to the real-world INFECTIOUS dataset¹ (Isella et al., 2011), which records temporal social interactions as dynamic networks. The data were collected at the Science Gallery in Dublin, where participants wore proximity sensors, and an edge was logged whenever a face-to-face interaction lasted more than 20 seconds.

Each day’s data yield a time-indexed network in which nodes represent individuals and edges denote interactions. We focus on a single day—June 28, 2009—aggregating the data into 30-minute windows to produce 12 networks. The connected components of each graph induce an unlabelled partition representing clusters of individuals in contact. Fig. 1 in Section 1 displays four representative networks, each inducing partitions $(11, 9, 4, 3)$, $(38, 2)$, $(22, 3, 2, 2, 2)$, and $(17, 4, 2, 2, 2)$.

We model the time-varying group structure using a two-parameter Poisson–Dirichlet diffusion for the latent probabilities of cluster sizes. Our inferential target is the heterozygosity functional $H_2(x) := 1 - \sum_{j \geq 1} x_j^2$, which approximates the probability that two randomly chosen individuals belong to different components, serving as a proxy for effective population mixing and epidemic spread.

Fig. 10 reports posterior estimates of $H_2(x)$ across time. Filtering and smoothing are implemented using the marginal MLEs $(\hat{\alpha}, \hat{\theta}) = (0, 0.75)$ obtained as in Section 4.3. As expected, smoothing provides sharper uncertainty quantification due to backward information flow, while filtering offers a real-time alternative with competitive accuracy.

As in Section 4.4, we contrast these results with two commonly used alternatives: the bootstrap particle filter and independent priors fitted separately at each time point. The former produces more dispersed posteriors and occasional multimodality (e.g., at t_5), while the latter suffers from inflated uncertainty and instability due to the lack of temporal structure. Further details are provided in Section A.5.3.

In terms of computational efficiency, our duality-based filter completes posterior sampling in under two minutes on a standard laptop, while the bootstrap particle filter takes approximately one hour due to path simulation and repeated evaluation of an intractable likelihood (3). This highlights the practical advantages of exploiting the discrete dual process for inference in complex time-evolving systems.

¹<http://www.sociopatterns.org/datasets/infectious-sociopatterns/>

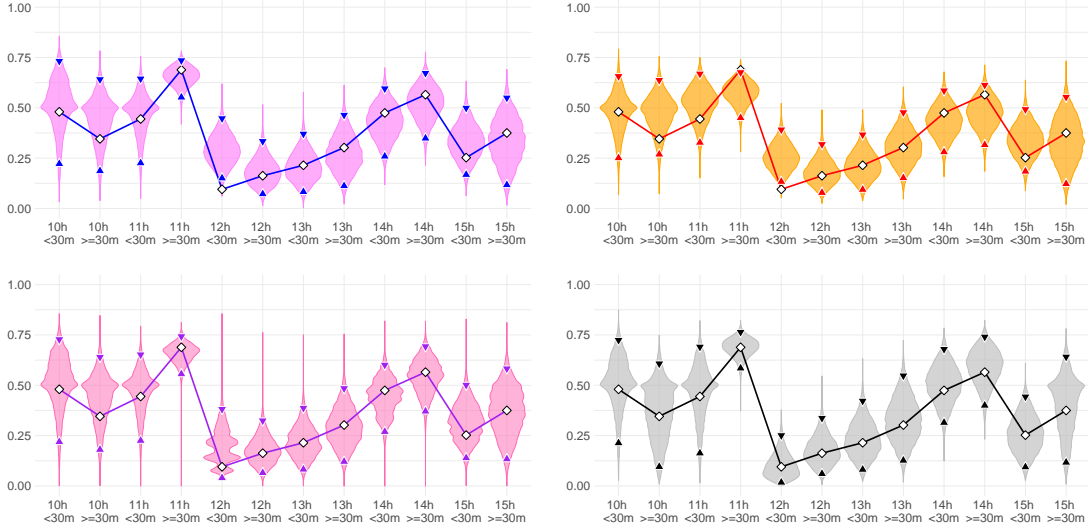


Figure 10: Top: online filtering (left) and offline smoothing (right) of heterozygosity for the INFECTIOUS dataset. Bottom: corresponding posteriors from a bootstrap particle filter (left) and independent priors (right). Violin plots: posterior densities; triangles: 95% credible intervals; white diamonds: observed heterozygosities. All methods use global MLEs ($\hat{\alpha}, \hat{\theta}$) except the independent prior approach, which estimates them separately at each time point.

5 Concluding remarks

We developed an exact and tractable inferential framework for nonparametric hidden Markov models where the latent process is a two-parameter Poisson–Dirichlet diffusion and the observations are unlabelled partitions evolving over discrete time. By exploiting Markov duality and combinatorial properties of partition coagulations, we derived recursive updates for both posterior and predictive distributions. These results enabled exact filtering, smoothing, and forecasting algorithms, as well as marginal likelihood-based parameter estimation.

Our approach demonstrates practical scalability and statistical fidelity in modeling time-varying unlabelled partition data. Unlike conventional particle filters, which require simulating high-dimensional latent dynamics and evaluating intractable likelihoods, our method sidesteps both difficulties through structural duality and quasi-conjugacy. The resulting algorithms are not only substantially faster, reducing runtime from approximately one hour to under two minutes, but also more stable, yielding coherent posterior trajectories and sharper uncertainty quantification. As shown through synthetic and real-world experiments, the proposed methodology enables tractable, interpretable, and provably exact inference in settings where the latent structure is infinite-dimensional and only partially observed. These properties make it particularly well suited for applications with computational constraints or unobserved individual-level labels, such as social or genetic data.

A Appendix

A.1 Two-parameter Poisson–Dirichlet diffusions

The two-parameter Poisson–Dirichlet diffusion takes values in the closure of the infinite-dimensional ordered simplex, sometimes called Kingman simplex, defined as

$$\bar{\nabla} = \left\{ x \in [0, 1]^\infty : x_1 \geq x_2 \geq \dots \geq 0, \sum_{i=1}^{\infty} x_i \leq 1 \right\},$$

which is a compact space in the product topology. Its infinitesimal operator is defined, for $\alpha \in [0, 1)$ and $\theta \geq -\alpha$.

$$A = \frac{1}{2} \sum_{i,j=1}^{\infty} x_i (\delta_{ij} - x_j) \frac{\partial^2}{\partial x_i \partial x_j} - \frac{1}{2} \sum_{i=1}^{\infty} (\theta x_i + \alpha) \frac{\partial}{\partial x_i},$$

with domain given by the subalgebra of the space $C(\bar{\nabla})$ of continuous function on $\bar{\nabla}$ generated by $\{\varphi_m(x), m \in \mathbb{N}\}$, with $\varphi_1(x) \equiv 1$ and $\varphi_m(x) = \sum_{i=1}^{\infty} x_i^m$ for $m \geq 2$. See, e.g., Feng (2010), Section 5.5. The transition function of the diffusion was found in Feng et al. (2011) through a spectral expansion, and admits the representation as infinite mixture of conditional two-parameter Poisson–Dirichlet distributions

$$p_t(x, \cdot) = (d_0(t) + d_1(t)) \text{PD}_{\alpha, \theta}(\cdot) + \sum_{n \geq 2} d_n(t) \sum_{\pi: |\pi|=n} P(\pi|x) \text{PD}_{\alpha, \theta}^{\pi}(\cdot). \quad (13)$$

See Griffiths et al. (2024) for a discussion. Here $P(\pi|x)$ is

$$P(\pi|x) := C(\pi) \sum_{i_1 \neq \dots \neq i_d} x_{i_1}^{\pi_1} x_{i_2}^{\pi_2} \dots x_{i_d}^{\pi_d}. \quad (14)$$

and $\text{PD}_{\alpha, \theta}^{\pi}$ is the law of a two-parameter Poisson–Dirichlet random probability measure conditional on a partition π (cf. Sec. 3.1). Furthermore,

$$d_n^{\theta}(t) = \sum_{k=n}^{\infty} e^{-k(\theta+k-1)t/2} (-1)^{k-n} \frac{(2k+\theta-1)(\theta+n)(k-1)}{n!(k-n)!}, \quad (15)$$

where $a_{(m)} = a(a+1)\dots(a+m+1)$ is the ascending factorial or Pochhammer symbol, with $a_{(0)} := 1$. These $d_n(t)$ are the transition probabilities of a death process on $\mathbb{Z}_+ = \{0, 1, \dots\}$ that has entrance boundary at ∞ and infinitesimal transition rates $n(\theta+n-1)/2$ from n to $n-1$. This process is in fact the *block-counting process* associated to Kingman’s coalescent with mutation (Tavaré, 1984).

It was showed by Ethier (2014) that, almost surely, the two-parameter diffusion takes values in

$$\nabla = \left\{ x \in [0, 1]^\infty : x_1 \geq x_2 \geq \dots \geq 0, \sum_{i=1}^{\infty} x_i = 1 \right\}$$

at all $t > 0$, so that $\overline{\nabla} \setminus \nabla$ acts as an entrance boundary. Then, if $X(0) \in \nabla$ almost surely, we can take ∇ as the process state space. For this reason we assumed $X(0) \sim \text{PD}_{\alpha,\theta}$, which implies $X(0) \in \nabla$ with probability one (Pitman, 2006).

A.2 Coagulation of random partitions

A.2.1 Two-parameter Poisson–Dirichlet partition structures

An integer *partition* of $n \in \mathbb{N}$ is a nonincreasing vector $\pi = (\pi_1, \dots, \pi_{l(\pi)})$ of positive integers with $|\pi| := \sum_{i=1}^{l(\pi)} \pi_i = n$. See Figure 2 for examples of Young diagram representation of partitions. Let \mathcal{P}_n be the set of partitions of n and $\mathcal{P} := \bigcup_{n \geq 1} \mathcal{P}_n$. For $\pi \in \mathcal{P}$, write $a(\pi) := (a_j(\pi), j \geq 1)$ where

$$a_j(\pi) := \sum_{i=1}^{l(\pi)} \mathbb{1}\{\pi_i = j\} \quad (16)$$

is the multiplicity of part size j . We partially order \mathcal{P} by $\pi \preccurlyeq \lambda$ if the Young diagram of π is obtained from that of λ by deleting squares; for $\Lambda \subseteq \mathcal{P}$, define the *lower set* $L(\Lambda) := \{\pi : \pi \preccurlyeq \lambda, \lambda \in \Lambda\}$. A *partition structure* (Kingman, 1978) is a family $\{P_n : n \in \mathbb{N}\}$ with P_n a probability on \mathcal{P}_n such that P_n is the marginal obtained by removing uniformly at random one square from the Young diagram of $\Pi \sim P_{n+1}$.

Throughout we use the Ewens–Pitman (α, θ) partition structure (Pitman, 1995, 2006). Its mass function $\text{PSF}_{\alpha,\theta}(\pi)$ is given in the main text at (1); the associated combinatorial coefficient is

$$C(\pi) = \binom{|\pi|}{\pi_1, \dots, \pi_{l(\pi)}} \frac{1}{a_1(\pi)! \cdots a_{|\pi|}(\pi)!}, \quad (17)$$

and we use the rising factorial notation $q_{(b)} := q(q+1) \cdots (q+b-1)$ (with the convention $q_{(0)} := 1$). A random partition Π of size n with pmf $\{\text{PSF}_{\alpha,\theta}(\pi), \pi \in \mathcal{P}_n\}$ is denoted $\Pi \sim \text{CRP}(n)$. Equivalently, Π can be generated by the (α, θ) Chinese restaurant process (CRP): the i th item joins an existing block of current size n_j with probability $(n_j - \alpha)/(\theta + i - 1)$, or starts a new block with probability $(\theta + \alpha K)/(\theta + i - 1)$, where K is the current number of blocks.

A.2.2 Coagulation of two-parameter random partitions

A key ingredient in our framework is the *coagulation* of partitions. Informally, given $\omega, \gamma \in \mathcal{P}$, a coagulation is obtained by summing selected pairs of parts and appending the remainder.

Recall that a *composition* is an unordered partition, and a *weak composition* allows zeros. The following makes Definition 2 in the main text explicit.

Definition 3 (Coagulation of partitions). *Let $\omega, \gamma \in \mathcal{P}$ and $0 \leq d \leq \min(l(\omega), l(\gamma))$. For compositions z, y of length d with $a(z) \leq a(\omega)$ and $a(y) \leq a(\gamma)$, with $a(\cdot)$ as in (16), define*

$$a(\mu) = a(z + y) + a(\omega) - a(z) + a(\gamma) - a(y),$$

where $\mu \in \mathcal{P}_{|\omega|+|\gamma|}$. The coagulation of ω and γ is

$$\text{coag}(\omega, \gamma) := \bigcup_{d=0}^{\min(l(\omega), l(\gamma))} \bigcup_{z,y} \text{coag}_{z,y}(\omega, \gamma),$$

with the setwise extension $\text{coag}(\Omega, \Gamma) := \bigcup_{\omega \in \Omega, \gamma \in \Gamma} \text{coag}(\omega, \gamma)$.

See Figure 2. Different choices of z, y may yield the same coagulation. This operation is crucial for describing products of likelihoods as in (14).

Proposition 4. *Let $x \in \nabla$, $\omega \in \mathcal{P}_n$, $\gamma \in \mathcal{P}_m$, and $P(\cdot|x)$ as in (14). Then*

$$P(\omega|x)P(\gamma|x) = \sum_{\mu \in \text{coag}(\omega, \gamma)} \mathcal{H}(\omega, \gamma|\mu) P(\mu|x),$$

where

$$\mathcal{H}(\omega, \gamma|\mu) = \binom{n+m}{n, m}^{-1} \sum \prod_{j=1}^{l(\mu)} \binom{\mu_j}{z_j, y_j},$$

and the sum runs over weak compositions z, y of n, m consistent with ω, γ .

Proposition 4 underpins quasi-conjugacy: while products of likelihoods exit the family, they remain finite linear combinations of the same kernels, corresponding to coagulated partitions.

Proposition 5. *For $\omega \in \mathcal{P}_n$, $\gamma \in \mathcal{P}_m$, $\mu \in \text{coag}(\omega, \gamma)$,*

$$\Pr(\Pi_{1:n+m} = \mu, \Pi_{n+1:n+m} = \gamma \mid \Pi_{1:n} = \omega) = \mathcal{H}(\omega, \gamma|\mu) \frac{\text{PSF}_{\alpha, \theta}(\mu)}{\text{PSF}_{\alpha, \theta}(\omega)}.$$

Integrating over μ in the statement of Proposition 5 yields

$$\text{CRP}_{\omega \uparrow \gamma} := \Pr(\Pi_{n+1:n+m} = \gamma \mid \Pi_{1:n} = \omega) = \sum_{\mu \in \text{coag}(\omega, \gamma)} \mathcal{H}(\omega, \gamma|\mu) \frac{\text{PSF}_{\alpha, \theta}(\mu)}{\text{PSF}_{\alpha, \theta}(\omega)}, \quad (18)$$

the conditional CRP kernel. Moreover,

$$\Pr(\Pi_{1:n+m} = \mu \mid \Pi_{1:n} = \omega, \Pi_{n+1:n+m} = \gamma) \propto \mathcal{H}(\omega, \gamma|\mu) \text{PSF}_{\alpha, \theta}(\mu), \quad \mu \in \text{coag}(\omega, \gamma) \quad (19)$$

and we will write $\Pi_{1:n+m} \mid \Pi_{1:n} = \omega, \Pi_{n+1:n+m} = \gamma \sim \text{Coag}_{\alpha, \theta}(\omega, \gamma)$, the coagulation kernel. Finally, conditional on $\Pi_{n+1:n+m} = \pi$, any prior distribution v_ω over ω is updated as

$$\hat{v}_\omega \propto v_\omega \text{CRP}_{\omega \uparrow \pi},$$

and the joint law of $\Pi_{1:n+m}$ is a mixture of coagulation kernels:

$$\Pi_{1:n+m} \mid \Pi_{n+1:n+m} = \pi \sim \sum_{\omega} \hat{v}_\omega \text{Coag}_{\alpha, \theta}(\omega, \pi). \quad (20)$$

This sequential structure will be the basis for filtering $\text{PD}_{\alpha, \theta}$ diffusions given partition-valued observations.

A.3 A CRP with loss of particles as dual process

Two Markov processes $X = (X(t); t \geq 0)$ and $D = (D(t); t \geq 0)$ with state spaces \mathcal{X}, \mathcal{D} are said to be *dual* with respect to a bounded measurable function $H : \mathcal{X} \times \mathcal{D} \rightarrow \mathbb{R}$ if

$$\mathbb{E}[H(X(t), d) \mid X(0) = x] = \mathbb{E}[H(x, D(t)) \mid D(0) = d].$$

See Jansen and Kurt (2014) for background.

Griffiths et al. (2024) showed that the dual process of the two-parameter Poisson–Dirichlet diffusion is a continuous-time Markov chain on partitions \mathcal{P} , with transition kernel

$$p_{\lambda, \omega}^{\downarrow}(t) := \Pr(D(t) = \omega \mid D(0) = \lambda) = \mathcal{H}(\omega \mid \lambda) d_{|\lambda|, |\omega|}^{\theta}(t), \quad \omega \in L(\lambda), \quad (21)$$

where $H(x, \omega) = P(\omega \mid x)/\text{PSF}_{\alpha, \theta}(\omega)$, $\mathcal{H}(\omega \mid \lambda)$ is obtained by integrating out γ from the symmetrized hypergeometric coefficient in Proposition 4, and $d_{n, m}^{\theta}(t)$ is the transition probability of the block-counting process of Kingman’s coalescent. Thus the dual is a *pure-death process* on integer partitions: from state λ , jumps occur at rate $|\lambda|(|\lambda| + \theta - 1)/2$, and a uniformly chosen square from the Young diagram of λ is deleted. A random partition with law (21) will be denoted $\Pi \sim p_{\lambda, \bullet}^{\downarrow}(t)$. As in (20), mixtures of dual processes arise naturally. If the initial state is random with distribution $\{w_{\lambda}, \lambda \in \mathcal{P}\}$, then

$$\Pi \sim \sum_{\lambda} w_{\lambda} p_{\lambda, \bullet}^{\downarrow}(t)$$

is the distribution of the dual process started from this mixture.

This dual representation is central to our methodology: it enables tractable filtering of a two-parameter Poisson–Dirichlet hidden Markov model, with the random loss of particles in the dual mirroring the contraction of information through time in the latent diffusion.

A.4 Details and proofs on filtering and smoothing

A.4.1 Online estimation: filtering and prediction

We introduce two operators mapping probability measures on ∇ into themselves.

The first is the *propagation operator*

$$\varphi_t(\nu)(dx') = \nu \mathcal{T}_t(dx') := \int_{\nabla} \nu(dx) p_t(x, dx'), \quad \mathcal{T}_t f(x) := \int_{\nabla} f(x') p_t(x, dx'), \quad (22)$$

where $\{\mathcal{T}_t, t \geq 0\}$ is the semigroup of the $\text{PD}_{\alpha, \theta}$ diffusion with transition kernel $p_t(x, dx')$. While p_t admits only an infinite mixture expansion (cf. (13)), we will see that $\varphi_t(\nu)$ is finite whenever ν is. The second operator, denoted ϕ_{π} , acts as a Bayesian update: if $X(t_k) \sim \nu$, then $\phi_{\pi}(\nu)$ is the law of $X(t_k) \mid \Pi^k = \pi$.

Starting from $X(t_0) \sim \text{PD}_{\alpha, \theta}$, the filtering recursion is

$$\nu_{0|0} := \phi_{\Pi^0}(\text{PD}_{\alpha, \theta}), \quad \nu_{k|0:k} = \phi_{\Pi^k}(\varphi_{\Delta_k}(\nu_{k-1|0:k-1})), \quad \Delta_k := t_k - t_{k-1}. \quad (23)$$

Propagation. Suppose $\nu_{k-1|0:k-1} = \sum_{\lambda \in \Lambda_{0:k-1}} w_\lambda \text{PD}_{\alpha,\theta}^\lambda$. Propagation over Δ_k yields:

Theorem 2 (Propagation). *The predictive law $\nu_{k|0:k-1}$ of $X(t_k) \mid \Pi^{0:k-1}$ belongs to \mathcal{F} :*

$$X(t_k) \mid \lambda(t_k) \sim \text{PD}_{\alpha,\theta}^{\lambda(t_k)}, \quad \lambda(t_k) \sim \sum_{\lambda \in \Lambda_{0:k-1}} w_\lambda p_{\lambda,\bullet}^\downarrow(\Delta_k), \quad (24)$$

where $p_{\lambda,\bullet}^\downarrow(\Delta_k)$ are the dual transition probabilities (21). Equivalently,

$$\nu_{k|0:k-1} = \sum_{\omega \in L(\Lambda_{0:k-1})} v_\omega \text{PD}_{\alpha,\theta}^\omega, \quad v_\omega = \sum_{\lambda \in \Lambda_{0:k-1}} w_\lambda p_{\lambda,\omega}^\downarrow(\Delta_k).$$

This shows that although the transition density of the $\text{PD}_{\alpha,\theta}$ diffusion is an doubly infinite sum (cf. (13) and (15)), its effect on finite mixtures is finite. Sampling proceeds as follows:

1. draw $\lambda(t_{k-1}) \sim \{w_\lambda\}$,
2. draw $\lambda(t_k) \sim p_{\lambda(t_{k-1}),\bullet}^\downarrow(\Delta_k)$,
3. draw $X(t_k) \sim \text{PD}_{\alpha,\theta}^{\lambda(t_k)}$.

An important corollary is convergence to stationarity: for $t \rightarrow \infty$, $\varphi_t(\nu_{N|0:N}) \rightarrow \text{PD}_{\alpha,\theta}$ in total variation.

Corollary 1. *Let $\varphi_t(\nu_{N|0:N})(\cdot) := \Pr_{\alpha,\theta}(X(t_N + t) \in \cdot \mid \Pi^{0:N})$. Then*

$$\varphi_t(\nu_{N|0:N}) \rightarrow \text{PD}_{\alpha,\theta},$$

in total variation, as $t \rightarrow \infty$.

Update. Given $\Pi^k = \pi^k$, we condition $\nu_{k|0:k-1}$ to obtain:

Theorem 3 (Update). *If $\nu_{k|0:k-1} = \sum_{\omega \in L(\Lambda_{0:k-1})} v_\omega \text{PD}_{\alpha,\theta}^\omega$, then*

$$X(t_k) \mid \lambda(t_k) \sim \text{PD}_{\alpha,\theta}^{\lambda(t_k)}, \quad \lambda(t_k) \mid \pi^k \sim \sum_{\omega \in L(\Lambda_{0:k-1})} \hat{v}_\omega \text{Coag}_{\alpha,\theta}(\omega, \pi^k), \quad (25)$$

with $\hat{v}_\omega \propto v_\omega \text{CRP}_{\omega \uparrow \pi^k}$, where $\text{CRP}_{\omega \uparrow \pi^k}$ is in (4) and $\text{Coag}_{\alpha,\theta}$ as in (19). Equivalently,

$$\nu_{k|0:k} = \sum_{\lambda \in \Lambda_{0:k}} w_\lambda \text{PD}_{\alpha,\theta}^\lambda, \quad w_\lambda \propto \sum_{\omega \in L(\Lambda_{0:k-1})} \hat{v}_\omega \Pr(\lambda \mid \omega, \pi^k),$$

with $\Lambda_{0:k} = \text{coag}(L(\Lambda_{0:k-1}), \pi^k)$.

The result follows because $P(\pi^k \mid x)$ can be factorized kernel by kernel in $\nu_{k|0:k-1}$, and Proposition 4 expresses the resulting product as a mixture over coagulations.

Filtering algorithm. Theorems 2 and 3 yield an exact recursive filtering scheme for the HMM (5), summarized in Algorithm 6. Practical aspects, including approximation strategies, are discussed in Section A.5.

A.4.2 Offline estimation: smoothing and data forecasting

After observing $\Pi^{0:N}$, we (i) refine state estimates at past observation times and (ii) generate future or interpolated data. For $k \leq N$, define the *marginal smoother*

$$\nu_{k|0:N}(A) := \Pr(X(t_k) \in A \mid \Pi^{0:N}).$$

Backward information (cost-to-go). Define

$$\Pr(\Pi^{k:N} \mid X(t_{k-1}) = x)$$

as the likelihood of the remaining partitions $\Pi^{k:N}$ given the state at t_{k-1} . This quantity, also known as the *cost-to-go function* or *backward information filter*, admits a general recursive representation. For intuition, in the simplest case $k = N$ one obtains

$$\Pr(\Pi^N = \pi \mid X(t_{N-1}) = x) = \text{PSF}_{\alpha,\theta}(\pi) \sum_{\lambda \in L(\pi)} h_\lambda(\Delta_N) \frac{P(\lambda \mid x)}{\text{PSF}_{\alpha,\theta}(\lambda)}, \quad \pi \in \mathcal{P}_{n_N},$$

where $h_\lambda(\Delta_N)$ is a distribution on $L(\pi)$. The sum is finite (cf. Fig. 4).

The general form is as follows.

Proposition 6 (Cost-to-go). *Let $\Pi^{0:N} = \pi^{0:N}$ be the observed partitions. Then*

$$\Pr(\Pi^k = \pi^k, \dots, \Pi^N = \pi^N \mid X(t_{k-1}) = x) = \prod_{j=k}^N g(\pi^j \mid \pi^{j+1:N}) \sum_{\omega \in \Omega^{k:N}} h_\omega(\Delta_k) \frac{P(\omega \mid x)}{\text{PSF}_{\alpha,\theta}(\omega)},$$

where

$$g(\pi^N) = \text{PSF}_{\alpha,\theta}(\pi^N), \quad h_\omega(\Delta_N) = p_{\pi^N, \omega}^\downarrow(\Delta_N), \quad \omega \in \Omega^{N:N},$$

and for $k = 1, \dots, N-1$,

$$g(\pi^k \mid \pi^{k+1:N}) = \sum_{\omega \in \Omega^{k+1:N}} h_\omega(\Delta_{k+1}) \text{CRP}_{\omega \uparrow \pi^k}.$$

The backward weights $h_\omega(\Delta_k)$ are computed recursively via

$$h_\omega(\Delta_k) = \sum_{\mu \in \text{coag}(\Omega^{k+1:N}, \pi^k)} \left[\sum_{\omega' \in \Omega^{k+1:N}} \frac{h_{\omega'}(\Delta_{k+1}) \text{CRP}_{\omega' \uparrow \pi^k}}{g(\pi^k \mid \pi^{k+1:N})} \Pr(\mu \mid \omega', \pi^k) \right] p_{\mu, \omega}^\downarrow(\Delta_k),$$

with $\text{CRP}_{\omega' \uparrow \pi^k}$ as in (18) and $\Pr(\mu \mid \omega', \pi^k)$ as in (19).

Forward and backward supports. To combine forward and backward information, we define two deterministic sets of partitions. The forward support $\Lambda_{0:k}$ is the set of partitions that carry positive mass after filtering up to time t_k (Theorems 2, 3). The backward supports are defined recursively from the observed data:

$$\Omega^{N:N} := L(\pi^N), \quad \Omega^{k:N} := L(\text{coag}(\Omega^{k+1:N}, \pi^k)), \quad k = N-1, \dots, 0,$$

with $L(\cdot)$ and $\text{coag}(\cdot, \cdot)$ as in Sections A.2.1 and A.2.2. Intuitively, $\Lambda_{0:k}$ encodes forward uncertainty up to t_k , while $\Omega^{k:N}$ encodes backward constraints imposed by future data.

Having both components, we can now combine them to obtain the full smoothing distribution.

Theorem 4 (Smoothing). *For $k = 0, \dots, N$, the smoothed law of $X(t_k) \mid \Pi^{0:N}$ belongs to \mathcal{F} and can be written as*

$$X(t_k) \mid \lambda(t) \sim \text{PD}_{\alpha, \theta}^{\lambda(t)}, \quad \lambda(t) \mid \Pi^{0:N} \sim \sum_{(\lambda, \omega) \in \Lambda_{0:k} \times \Omega^{k:N}} w_{\lambda, \omega} \text{Coag}_{\alpha, \theta}(\lambda, \omega),$$

where

$$w_{\lambda, \omega} \propto v_{\lambda} \frac{\Pr(\Pi_{1:|\lambda|} = \lambda, \Pi_{|\lambda|+1:|\lambda|+|\omega|} = \omega)}{\text{PSF}_{\alpha, \theta}(\lambda) \text{PSF}_{\alpha, \theta}(\omega)} h_{\omega},$$

v_{λ} are the forward weights on $\Lambda_{0:k}$ (Theorem 2), and h_{ω} are the backward weights on $\Omega^{k:N}$ from Proposition 6. See Section A.4.3 for the proof and Section A.5.2 for further discussion.

Algorithm 7 evaluates $\nu_{k|0:N}$ by combining the forward mixture at t_k with the backward information summarized by $\Omega^{k:N}$ via coagulation.

Interpolation between observation times. The same structure yields $\Pr(X(t_k + \delta) \in \cdot \mid \Pi^{0:N})$ for $0 < \delta < \Delta_{k+1}$.

Corollary 2 (Interpolation). *For $t_k + \delta \in (t_k, t_{k+1})$, $\Pr(X(t_k + \delta) \in dx \mid \Pi^{0:N}) \in \mathcal{F}$ and*

$$\Pr(X(t_k + \delta) \in dx \mid \Pi^{0:N}) = \sum_{\mu \in \text{coag}(L(\Lambda_{0:k}), \Omega^{k:N})} s_{\mu}(\delta, \Delta_{k+1}) \text{PD}_{\alpha, \theta}^{\mu}(dx),$$

with (up to normalization)

$$s_{\mu}(\delta, \Delta_{k+1}) \propto \sum_{\eta \in L(\Lambda_{0:k})} \sum_{\omega \in \Omega^{k:N}} w_{\eta, \omega}(\delta, \Delta_{k+1}) \Pr(\mu \mid \eta, \omega),$$

$$w_{\eta, \omega}(\delta, \Delta_{k+1}) \propto w_{\eta}(\delta) \frac{\Pr(\Pi_{1:|\eta|} = \eta, \Pi_{|\eta|+1:|\eta|+|\omega|} = \omega)}{\text{PSF}_{\alpha, \theta}(\eta) \text{PSF}_{\alpha, \theta}(\omega)} h_{\omega}(\Delta_{k+1} - \delta),$$

where $w_{\eta}(\delta)$ are the forward propagation weights over δ (Theorem 2) and $h_{\omega}(\cdot)$ are cost-to-go weights (Proposition 6).

For $t > t_N$, use the forecast $\varphi_{t-t_N}(\nu_{N|0:N})$ (Theorem 2 and Corollary 1).

Forecasting new partition data. We can also simulate future (or interpolated) partitions $\Pi'(t)$ of size n conditional on $\Pi^{0:N}$.

Corollary 3 (Forecasting partitions). *For any $t \geq 0$ under (5),*

$$\Pi'(t) \mid \lambda(t) \sim \text{CRP}_{\lambda(t) \uparrow \bullet}, \quad \lambda(t) \sim \{w_\lambda\}, \quad (26)$$

where $\{w_\lambda\}$ are the mixture weights for $\Pr(X(t) \in dx \mid \Pi^{0:N})$, obtained from: Theorem 2 if $t > t_N$; Theorem 3 if $t = t_N$; Theorem 4 if $t = t_k < t_N$; or Corollary 2 if $t \in (t_k, t_{k+1})$.

Algorithm 8 then samples Young diagrams conditionally on $\pi^{0:N}$. Equation (26) can be seen as a temporally informed CRP, where temporal dependence is encoded by the weights $\{w_\lambda\}$; the overall clustering structure is unknown within the finite set of plausible coagulations.

A.4.3 Proofs

Proof of Proposition 4. We give here a direct probabilistic proof which highlights the role of the random sampling. See also Feng et al. (2011); Feng (2010) for previous discussion of similar results. By (14), we can write

$$P(\omega|x)P(\gamma|x) = \Pr_x(\Pi_{1:n} = \omega, \Pi_{n+1:n+m} = \gamma)$$

which factorizes since the two samples are conditionally independent given x . By construction, $\Pr_x(\Pi_{1:n} = \omega, \Pi_{n+1:n+m} = \gamma \mid \Pi_{1:n+m} = \mu)$ is in fact independent of x and coincides with the sum of joint hypergeometric probabilities in (4). Then

$$\begin{aligned} \Pr_x(\Pi_{1:n} = \omega, \Pi_{n+1:n+m} = \gamma) &= \sum_{\mu \in \mathcal{P}_{n+m}} \Pr_x(\Pi_{1:n} = \omega, \Pi_{n+1:n+m} = \gamma, \Pi_{1:n+m} = \mu) \\ &= \sum_{\mu \in \mathcal{P}_{n+m}} \Pr_x(\Pi_{1:n+m} = \mu) \Pr_x(\Pi_{1:n} = \omega, \Pi_{n+1:n+m} = \gamma \mid \Pi_{1:n+m} = \mu) \\ &= \sum_{\mu \in \mathcal{P}_{n+m}} \Pr_x(\Pi_{1:n+m} = \mu) \mathcal{H}(\omega, \gamma \mid \mu) \end{aligned}$$

but $\mathcal{H}(\omega, \gamma \mid \mu) = 0$ if $\mu \notin \text{coag}(\omega, \gamma)$, i.e., if μ cannot be obtained as a coagulation of ω, γ , yielding the result. \square

Proof of Proposition 5. The law of a partition drawn from a two-parameter Chinese restaurant process can be written by integrating out the $\text{PD}_{\alpha, \theta}$ -distributed random measure, yielding the de Finetti representation

$$\begin{aligned} \Pr(\Pi_{n+1:n+m} = \gamma \mid \Pi_{1:n} = \omega) &= \int_{\nabla} P(\gamma|x) \text{PD}_{\alpha, \theta}^{\omega}(dx), \\ \text{PD}_{\alpha, \theta}^{\omega}(dx) &= \frac{P(\omega|x) \text{PD}_{\alpha, \theta}(dx)}{\text{PSF}_{\alpha, \theta}(\omega)}. \end{aligned} \quad (27)$$

Using (27), the left-hand side of Proposition 5 can be written as a mixture,

$$\begin{aligned} & \Pr(\Pi_{1:n+m} = \mu, \Pi_{n+1:n+m} = \gamma | \Pi_{1:n} = \omega) \\ &= \int_{\nabla} \Pr_x(\Pi_{1:n+m} = \mu, \Pi_{n+1:n+m} = \gamma | \Pi_{1:n} = \omega) \text{PD}_{\alpha,\theta}^\omega(dx). \end{aligned}$$

where \Pr_x denotes the law of random partitions induced by subsequent draws from $x \in \nabla$; cf. (14). Using (27), the previous equals

$$\int_{\nabla} \Pr_x(\Pi_{1:n+m} = \mu, \Pi_{n+1:n+m} = \gamma, \Pi_{1:n} = \omega) \frac{\text{PD}_{\alpha,\theta}^\omega(dx)}{\text{PSF}_{\alpha,\theta}^\omega(\omega)} \quad (28)$$

since $P(\omega|x) = \Pr_x(\Pi_{1:n} = \omega)$. Now, conditionally on $\Pi_{1:n+m}$ the subpartitions $\Pi_{1:n}$ and $\Pi_{n+1:n+m}$ are independent of x , (cf. proof of Proposition 4) and their conditional joint law is the hypergeometric in Proposition 4. Hence we have

$$\begin{aligned} & \Pr_x(\Pi_{1:n+m} = \mu, \Pi_{n+1:n+m} = \gamma, \Pi_{1:n} = \omega) \\ &= \Pr_x(\Pi_{1:n+m} = \mu) \Pr_x(\Pi_{n+1:n+m} = \gamma, \Pi_{1:n} = \omega | \Pi_{1:n+m} = \mu) \\ &= \Pr_x(\Pi_{1:n+m} = \mu) \mathcal{H}(\omega, \gamma | \mu), \end{aligned}$$

from which (28) becomes

$$\frac{\mathcal{H}(\omega, \gamma | \mu)}{\text{PSF}_{\alpha,\theta}^\omega(\omega)} \int_{\nabla} \Pr_x(\Pi_{1:n+m} = \mu) \text{PD}_{\alpha,\theta}^\omega(dx),$$

and the claim is now implied by Kingman's representation theorem (Kingman, 1978; Pitman, 1995). \square

Proof of Theorem 2. From (22) we have

$$\begin{aligned} \nu_{k|0:k-1}(dx) &= \varphi_{\Delta_k}(\nu_{k-1|0:k-1})(dx) = \int_{\nabla} \nu_{k-1|0:k-1}(dz) p_{\Delta_k}(z, dx) \\ &= \sum_{\lambda \in \Lambda} w_{\lambda} \int_{\nabla} \text{PD}_{\alpha,\theta}^{\lambda}(dz) p_{\Delta_k}(z, dx). \end{aligned}$$

Using now (27), the previous yields

$$\sum_{\lambda \in \Lambda} w_{\lambda} \int_{\nabla} \frac{P(\lambda|z)}{\text{PSF}_{\alpha,\theta}^{\lambda}(\lambda)} \text{PD}_{\alpha,\theta}^{\lambda}(dz) p_{\Delta_k}(z, dx).$$

Since the signal is reversible with respect to $\text{PD}_{\alpha,\theta}$ (cf. Petrov (2009), p. 280), using the detailed balance condition we obtain

$$\text{PD}_{\alpha,\theta}(dx) \sum_{\lambda \in \Lambda} w_{\lambda} \int_{\nabla} \frac{P(\lambda|z)}{\text{PSF}_{\alpha,\theta}^{\lambda}(\lambda)} p_{\Delta_k}(x, dz). \quad (29)$$

Due to the duality between the $\text{PD}_{\alpha,\theta}$ diffusion and the death process described in Section A.3, (29) becomes

$$\text{PD}_{\alpha,\theta}(\mathrm{d}x) \sum_{\lambda \in \Lambda} w_\lambda \mathbb{E}(H(x, D_{\Delta_k}) | D_0 = \lambda)$$

and since D_t is a death process on \mathcal{P} , we obtain

$$\text{PD}_{\alpha,\theta}(\mathrm{d}x) \sum_{\lambda \in \Lambda} w_\lambda \sum_{\omega \in L(\lambda)} \frac{P(\omega|x)}{\text{PSF}_{\alpha,\theta}(\omega)} p_{\lambda,\omega}^\downarrow(\Delta_k)$$

which upon a rearrangement and using again (27) yields the result. \square

Proof of Corollary 1. For any measurable $A \subset \nabla$, from (24) with $k = N$ and $t = \Delta_{N+1}$, we have

$$\begin{aligned} |\varphi_t(\nu_{N|0:N})(A) - \text{PD}_{\alpha,\theta}(A)| &\leq \sum_{\eta \in L(\Lambda)} v_\eta(t) \left| \text{PD}_{\alpha,\theta}^\omega(A) - \text{PD}_{\alpha,\theta}(A) \right| \\ &\leq v_\emptyset(t) \left| \text{PD}_{\alpha,\theta}(A) - \text{PD}_{\alpha,\theta}(A) \right| + v_{(1)}(t) \left| \text{PD}_{\alpha,\theta}^{(1)}(A) - \text{PD}_{\alpha,\theta}(A) \right| \\ &\quad + \sum_{\omega \in L(\Lambda_{0:N}): |\omega| > 1} v_\omega(t) \left| \text{PD}_{\alpha,\theta}^\omega(A) - \text{PD}_{\alpha,\theta}(A) \right|. \end{aligned}$$

Now, since

$$v_\omega(t) = \sum_{\lambda \in \Lambda_{0:N}} w_\lambda \mathcal{H}(\omega|\lambda) d_{|\lambda|,|\omega|}^\theta(t)$$

the fact that $d_{|\lambda|,|\omega|}^\theta(t)$ is the transition probability of a death-process in \mathbb{Z}_+ with absorption in (1) implies that $v_\omega(t) \rightarrow 0$ as $t \rightarrow \infty$ for all ω such that $|\omega| > 1$. The result is now implied by the fact that $\text{PD}_{\alpha,\theta}^{(1)} \xrightarrow{d} \text{PD}_{\alpha,\theta}$ (see Remark 1). \square

Proof of Theorem 3. An application of Bayes' theorem yields

$$\nu_{k|0:k}(\mathrm{d}x) \propto P(\pi^k|x) \nu_{k|0:k-1}(\mathrm{d}x),$$

so that substituting $\nu_{k|0:k-1}(\mathrm{d}x)$ as in Theorem 2 and using (27), we obtain

$$\sum_{\omega \in L(\Lambda_{0:k-1})} v_\omega P(\pi^k|x) P(\omega|x) \frac{\text{PD}_{\alpha,\theta}(\mathrm{d}x)}{\text{PSF}_{\alpha,\theta}(\omega)}.$$

Using now Propositions 4 and 5 leads to

$$\begin{aligned} &\sum_{\omega \in L(\Lambda_{0:k-1})} v_\omega \sum_{\mu \in \text{coag}(\omega, \pi^k)} \mathcal{H}(\omega, \pi^k|\mu) P(\mu|x) \frac{\text{PD}_{\alpha,\theta}(\mathrm{d}x)}{\text{PSF}_{\alpha,\theta}(\omega)} \\ &= \sum_{\omega \in L(\Lambda_{0:k-1})} v_\omega \sum_{\mu \in \text{coag}(\omega, \pi^k)} \mathcal{H}(\omega, \pi^k|\mu) \frac{\text{PSF}_{\alpha,\theta}(\mu)}{\text{PSF}_{\alpha,\theta}(\omega)} \text{PD}_{\alpha,\theta}^\mu(\mathrm{d}x) \end{aligned}$$

$$= \sum_{\omega \in L(\Lambda_{0:k-1})} v_\omega \sum_{\mu \in \text{coag}(\omega, \pi^k)} \Pr(\mu, \pi^k | \omega) \text{PD}_{\alpha, \theta}^\mu(\text{d}x).$$

Since the two sums are finite, we can normalize the last expression by

$$\sum_{\omega \in L(\Lambda_{0:k-1})} v_\omega \sum_{\mu \in \text{coag}(\omega, \pi^k)} \Pr(\mu, \pi^k | \omega) = \sum_{\omega \in L(\Lambda_{0:k-1})} v_\omega \text{CRP}_{\omega \uparrow \pi^k}$$

and multiply and divide by $\text{CRP}_{\omega \uparrow \pi^k}$ to obtain

$$\sum_{\omega \in L(\Lambda_{0:k-1})} \frac{v_\omega \text{CRP}_{\omega \uparrow \pi^k}}{\sum_{\omega'} v_{\omega'} \text{CRP}_{\omega' \uparrow \pi^k}} \sum_{\mu \in \text{coag}(\omega, \pi^k)} \Pr(\mu | \omega, \pi^k) \text{PD}_{\alpha, \theta}^\mu(\text{d}x).$$

A rearrangement leads to

$$\sum_{\mu \in \text{coag}(L(\Lambda_{0:k-1}), \pi^k)} \left[\sum_{\omega \in L(\Lambda_{0:k-1})} \hat{v}_\omega \Pr(\mu | \omega, \pi^k) \right] \text{PD}_{\alpha, \theta}^\mu(\text{d}x).$$

□

Proof of Proposition 6. Let us avoid to write the random partitions $\Pi^{k:N}$ in $\Pr_{\alpha, \theta}$ to ease the notation. We proceed by induction on k . First note that

$$\begin{aligned} \Pr(\pi^N | X(t_{N-1}) = x) &= \int_{\nabla} P(\pi^N | z) p_{\Delta_N}(x, \text{d}z) \\ &= \text{PSF}_{\alpha, \theta}(\pi^N) \int_{\nabla} \frac{P(\pi^N | z)}{\text{PSF}_{\alpha, \theta}(\pi^N)} p_{\Delta_N}(x, \text{d}z) \\ &= \text{PSF}_{\alpha, \theta}(\pi^N) \sum_{\omega \in \Omega^{N:N}} p_{\pi^N, \omega}^\downarrow(\Delta_N) \frac{P(\omega | x)}{\text{PSF}_{\alpha, \theta}(\omega)}, \end{aligned}$$

where in the last identity we have used the duality (recall Section A.3). Now, since

$$\begin{aligned} \Pr_{\alpha, \theta}(\pi^{k:N} | X(t_{k-1}) = x) &= \int_{\nabla} \Pr_{\alpha, \theta}(\pi^{k:N} | X(t_k) = z) p_{\Delta_k}(x, \text{d}z) \\ &= \int_{\nabla} P(\pi^k | z) \Pr_{\alpha, \theta}(\pi^{k+1:N} | X(t_k) = z) p_{\Delta_k}(x, \text{d}z), \end{aligned} \tag{30}$$

if we now assume

$$\Pr_{\alpha, \theta}(\pi^{k+1:N} | X(t_k) = x) = \prod_{j=k+1}^N g(\pi^j | \pi^{j+1:N}) \sum_{\omega \in \Omega^{k+1:N}} h_\omega(\Delta_{k+1}) \frac{P(\omega | x)}{\text{PSF}_{\alpha, \theta}(\omega)},$$

for some functions g and h_ω , then (30) equals

$$\prod_{j=k+1}^N g(\pi^j | \pi^{j+1:N}) \sum_{\omega \in \Omega^{k+1:N}} h_\omega(\Delta_{k+1}) \int_{\nabla} P(\pi^k | z) \frac{P(\omega | z)}{\text{PSF}_{\alpha, \theta}(\omega)} p_{\Delta_k}(x, \text{d}z).$$

Proposition 4 now gives

$$\prod_{j=k+1}^N g(\pi^j | \pi^{j+1:N}) \sum_{\substack{\omega \in \Omega^{k+1:N} \\ \mu \in \text{coag}(\pi^k, \omega)}} h_\omega(\Delta_{k+1}) \mathcal{H}(\pi^k, \omega | \mu) \frac{\text{PSF}_{\alpha, \theta}(\mu)}{\text{PSF}_{\alpha, \theta}(\omega)} \int_{\nabla} \frac{P(\mu | z)}{\text{PSF}_{\alpha, \theta}(\mu)} p_{\Delta_k}(x, dz)$$

and using the duality (recall Section A.3), we find

$$\prod_{j=k+1}^N g(\pi^j | \pi^{j+1:N}) \sum_{\substack{\omega \in \Omega^{k+1:N} \\ \mu \in \text{coag}(\pi^k, \omega)}} h_\omega(\Delta_{k+1}) \Pr(\mu, \pi^k | \omega) \sum_{\eta \preccurlyeq \mu} p_{\mu, \eta}^\downarrow(\Delta_k) \frac{P(\eta | x)}{\text{PSF}_{\alpha, \theta}(\eta)}.$$

The sums in the last display can be written

$$\sum_{\eta \in \Omega^{k:N}} \frac{P(\eta | x)}{\text{PSF}_{\alpha, \theta}(\eta)} \sum_{\mu \in \text{coag}(\pi^k, \Omega^{k+1:N})} p_{\mu, \eta}^\downarrow(\Delta_k) \sum_{\omega \in \Omega^{k+1:N}} h_\omega(\Delta_{k+1}) \Pr(\mu, \pi^k | \omega).$$

Now multiply and divide by

$$g(\pi^k | \pi^{k+1:N}) := \sum_{\omega \in \Omega^{k+1:N}} h_\omega(\Delta_{k+1}) \text{PSF}_{\alpha, \theta}(\pi^k | \omega)$$

and denote

$$h_\eta(\Delta_k) := \sum_{\mu \in \text{coag}(\pi^k, \Omega^{k+1:N})} \left[\sum_{\omega \in \Omega^{k+1:N}} \frac{h_\omega(\Delta_{k+1}) \text{CRP}_{\omega \uparrow \pi^k} \Pr(\mu | \omega, \pi^k)}{g(\pi^k | \pi^{k+1:N})} \right] p_{\mu, \eta}^\downarrow(\Delta_k),$$

which is the probability the dual process with initial distribution on $\text{coag}(\pi^k, \Omega^{k+1:N})$ given by the expression in square brackets is in state $\eta \in \Omega^{k:N}$ after a time interval equal to Δ_k . The induction is completed as we have found that

$$\Pr_{\alpha, \theta}(\pi^{k:N} | X(t_{k-1}) = x) = \prod_{j=k}^N g(\pi^j | \pi^{j+1:N}) \sum_{\omega \in \Omega^{k:N}} h_\omega(\Delta_k) \frac{P(\omega | x)}{\text{PSF}_{\alpha, \theta}(\omega)}.$$

□

Proof of Theorem 4. Consider first the following decomposition of the marginal smoothing distribution $\nu_{k|0:N}$,

$$\begin{aligned} \nu_{k|0:N}(A) &= \Pr_{\alpha, \theta}(X(t_k) \in A | \pi^{0:N}) \\ &\propto \int_A \Pr_{\alpha, \theta}(X(t_k) \in dx | \pi^{0:k}) \Pr_{\alpha, \theta}(\pi^{k+1:N} | X(t_k) = x) \\ &= \int_A \nu_{k|0:k}(dx) \Pr_{\alpha, \theta}(\pi^{k+1:N} | X(t_k) = x). \end{aligned} \tag{31}$$

where the random partitions $\Pi^{0:N}$ are not included in $\Pr_{\alpha,\theta}$ just to ease the notation. Hence, up to proportionality, $\nu_{k|0:N}$ factorizes into $\nu_{k|0:k}$ and the likelihood of partitions collected after time t_k , the latter given in Proposition 6. As the first factor in (31) is the filtering distribution $\nu_{k|0:k}$ in the statement, we now have

$$\nu_{k|0:N}(dx) \propto \sum_{\substack{\omega \in \Omega^{k:N} \\ \lambda \in \Lambda_{0:k}}} w_\lambda h_\omega(\Delta_{k+1}) \text{PD}_{\alpha,\theta}^\lambda(dx) \frac{P(\omega|x)}{\text{PSF}_{\alpha,\theta}(\omega)}.$$

Writing $\text{PD}_{\alpha,\theta}^\lambda(dx)$ as in (27) and applying Proposition 4 we get

$$\begin{aligned} \nu_{k|0:N}(dx) &\propto \sum_{\substack{\omega \in \Omega^{k:N} \\ \lambda \in \Lambda_{0:k}}} w_\lambda h_\omega(\Delta_{k+1}) \frac{P(\lambda|x)P(\omega|x)}{\text{PSF}_{\alpha,\theta}(\lambda)\text{PSF}_{\alpha,\theta}(\omega)} \text{PD}_{\alpha,\theta}(dx) \\ &= \sum_{\substack{\omega \in \Omega^{k:N} \\ \lambda \in \Lambda_{0:k}}} w_\lambda \frac{h_\omega(\Delta_{k+1})}{\text{PSF}_{\alpha,\theta}(\omega)} \sum_{\mu \in \text{coag}(\lambda,\omega)} \mathcal{H}(\lambda,\omega|\mu) \frac{P(\mu|x)}{\text{PSF}_{\alpha,\theta}(\lambda)} \text{PD}_{\alpha,\theta}(dx) \\ &= \sum_{\substack{\omega \in \Omega^{k:N} \\ \lambda \in \Lambda_{0:k}}} w_\lambda \frac{h_\omega(\Delta_{k+1})}{\text{PSF}_{\alpha,\theta}(\omega)} \sum_{\mu \in \text{coag}(\lambda,\omega)} \mathcal{H}(\lambda,\omega|\mu) \frac{\text{PSF}_{\alpha,\theta}(\mu)}{\text{PSF}_{\alpha,\theta}(\lambda)} \text{PD}_{\alpha,\theta}^\mu(dx) \\ &= \sum_{\substack{\omega \in \Omega^{k:N} \\ \lambda \in \Lambda_{0:k}}} w_\lambda \frac{h_\omega(\Delta_{k+1})}{\text{PSF}_{\alpha,\theta}(\omega)} \sum_{\mu \in \text{coag}(\lambda,\omega)} \Pr(\mu,\omega|\lambda) \text{PD}_{\alpha,\theta}^\mu(dx). \end{aligned}$$

where $\Pr(\mu,\omega|\lambda)$ is a shorthand notation for the conditional distribution in Proposition 5. Here the sums are finite, so inverting them leads to the mixture

$$\sum_{\mu \in \text{coag}(\Lambda^{0:k}, \Omega^{k:N})} \left[\sum_{\substack{\omega \in \Omega^{k:N} \\ \lambda \in \Lambda_{0:k}}} \frac{w_\lambda \text{CRP}_{\lambda \uparrow \omega} h_\omega(\Delta_{k+1})}{\text{PSF}_{\alpha,\theta}(\omega)} \Pr(\mu|\lambda,\omega) \right] \text{PD}_{\alpha,\theta}^\mu(dx),$$

which concludes the proof upon noting that $\Pr(\lambda,\omega) = \text{PSF}_{\alpha,\theta}(\lambda) \text{CRP}_{\lambda \uparrow \omega}$, which follows from (27). \square

Proof of Corollary 2. Following the same steps in the proof of Theorem 4,

$$\begin{aligned} \Pr_{\alpha,\theta}(X(t_k + \delta) \in dx | \pi^{0:N}) &\propto \Pr_{\alpha,\theta}(X(t_k + \delta) \in dx | \pi^{0:k}) \Pr_{\alpha,\theta}(\pi^{k+1:N} | X(t_k + \delta) = x) \\ &= \varphi_\delta(\nu_{0:k})(dx) \Pr_{\alpha,\theta}(\pi^{k+1:N} | X(t_k + \delta) = x). \end{aligned}$$

where the random partitions $\Pi^{0:N}$ are omitted in $\Pr_{\alpha,\theta}$ just to ease the notation. As already shown in Theorem 2, the propagation of $\nu_{k|0:k}$ is

$$\varphi_\delta(\nu_{k|0:k}) = \sum_{\omega \in L(\Lambda_{0:k})} v_\omega(\delta) \text{PD}_{\alpha,\theta}^\omega.$$

In order to find the likelihood $\Pr_{\alpha,\theta}(\pi^{k+1:N}|X(t_k + \delta) = x)$ one can proceed as in the proof of Proposition 6, but replacing $p_{\mu,\eta}^\downarrow(\Delta_{k+1})$ with $p_{\mu,\eta}^\downarrow(\Delta_{k+1} - \delta)$. \square

Proof of Corollary 3. The result is immediate upon writing the left-hand side of (26) as

$$\int_{\nabla} P(\pi|x) \Pr_{\alpha,\theta}(X(t) \in dx | \pi^{0:N}) = \sum_{\lambda \in \Lambda_t} w_\lambda \int_{\nabla} P(\pi|x) \text{PD}_{\alpha,\theta}^\lambda(dx)$$

and using (27). \square

A.5 Implementation

A.5.1 Pseudocodes

Algorithm 1: Sampling ε -PD $_{\alpha,\theta}$

Input: parameters α, θ ; truncation error $\varepsilon \in (0, 1)$

```

1  $r \leftarrow 1$ 
2  $i \leftarrow 0$ 
3 while  $r > \varepsilon$  do
4    $i \leftarrow i + 1$ 
5   Draw  $V_i \sim \text{Beta}(1 - \alpha, \theta + i\alpha)$ 
6    $X_i \leftarrow V_i \prod_{j < i} (1 - V_j)$ 
7    $r \leftarrow r - X_i$ 
8 return  $(X_1, \dots, X_i)$  in decreasing order (to be normalized if needed)

```

Algorithm 2: Sampling ε -PD $_{\alpha,\theta}^\pi$

Input: partition $\pi \in \mathcal{P}$, truncation error $\varepsilon \in (0, 1)$

```

1 Draw  $W \sim \text{Beta}(\theta + \alpha l(\pi), |\pi| - \alpha l(\pi))$ 
2 Draw  $X^{(1)} \sim \text{Dir}(\pi_1 - \alpha, \dots, \pi_{l(\pi)} - \alpha)$ 
3 Draw  $X^{(2)} \sim \text{PD}_{\alpha,\theta+\alpha l(\pi)}$  as in Algorithm 1 with truncation error  $\varepsilon/(1 - W)$ 
4 return  $((1 - W)X_1^{(1)}, \dots, (1 - W)X_{l(\pi)}^{(1)}, W X_1^{(2)}, W X_2^{(2)}, \dots)$  in decreasing order (to be normalized if needed)

```

Algorithm 3: Propagation – Sampling $X(t_k)$ given $\pi^{0:k-1}$ (exact)

Input: Active nodes $\Lambda \subset \mathcal{P}$ and weights $\{w_\lambda, \lambda \in \Lambda\}$ from $\nu_{k-1|0:k-1}$; sample size M

```

1 for  $\lambda \in \Lambda$  do
2   for  $\omega \preccurlyeq \lambda$  do
3     Initialization:  $v_\omega \leftarrow 0$  if  $v_\omega$  is NULL
4      $v_\omega \leftarrow v_\omega + w_\lambda p_{\lambda,\omega}^\downarrow(\Delta_k)$ 
5 Normalize  $\{v_\omega, \omega \in L(\Lambda)\}$ 
6 Draw  $\omega_m \sim v_\omega$  and  $X_m \sim \text{PD}_{\alpha,\theta}^{\omega_m}$  using Algorithm 2, for  $m = 1, \dots, M$ 
7 return  $\{v_\omega, \omega \in L(\Lambda)\}$  and  $\{X_m, m = 1, \dots, M\}$ 

```

Algorithm 4: Propagation – Sampling $X(t_k)$ given $\pi^{0:k-1}$ (Gillespie)

Input: Active nodes $\Lambda \subset \mathcal{P}$ and weights $\{w_\lambda, \lambda \in \Lambda\}$ from $\nu_{k-1|0:k-1}$; sample size M

- 1 **for** $m = 1, \dots, M$ **do**
- 2 Draw $\eta \sim w_\eta$
- 3 Draw $E \sim \text{Exp}(|\eta|(|\eta| + \theta - 1)/2)$
- 4 $\Delta \leftarrow E$
- 5 **while** $\Delta < \Delta_k$ **do**
- 6 Delete uniformly at random one square from the Young diagram of η
- 7 Draw $E \sim \text{Exp}(|\eta|(|\eta| + \theta - 1)/2)$
- 8 $\Delta \leftarrow \Delta + E$
- 9 Initialization: $v_\eta \leftarrow 0$ if v_η is NULL
- 10 $v_\eta \leftarrow v_\eta + 1$
- 11 Draw $X_m \sim \text{PD}_{\alpha, \theta}^\eta$ using Algorithm 2
- 12 **return** $\{v_\eta, \eta \in L(\lambda)\}$ normalized and $\{X_m, m = 1, \dots, M\}$

Algorithm 5: Update – Sampling $X(t_k)$ given $\pi^{0:k}$

Input: $\{w_\lambda, \lambda \in \Lambda\}$ from $\nu_{k|0:k-1}$; partition π^k ; sample size M

- 1 $\text{coag}(\Lambda, \pi^k) \leftarrow \emptyset$
- 2 **for** $\lambda \in \Lambda$ **do**
- 3 **for** $\mu \in \text{coag}(\Lambda, \pi^k)$ **do**
- 4 $\text{coag}(\Lambda, \pi^k) \leftarrow \text{coag}(\Lambda, \pi^k) \cup \mu$
- 5 Initialization: $v_\mu \leftarrow 0$ if v_μ is NULL
- 6 $v_\mu \leftarrow v_\mu + \frac{w_\lambda}{\text{PSF}_{\alpha, \theta}(\lambda)} \mathcal{H}(\lambda, \pi^k | \mu) \text{PSF}_{\alpha, \theta}(\mu)$
- 7 Normalize $\{v_\mu, \mu \in \text{coag}(\Lambda, \pi^k)\}$
- 8 Draw $\mu_m \sim v_\mu$ and $X_m \sim \text{PD}_{\alpha, \theta}^{\mu_m}$ using Algorithm 2, for $m = 1, \dots, M$
- 9 **return** $\{v_\mu, \mu \in \text{coag}(\Lambda, \pi^k)\}$ and $\{X_m, m = 1, \dots, M\}$

Algorithm 6: Filter

Input: Partitions $\pi^{0:N}$

- 1 **Update:** Let $\nu_{0|0} = \text{PD}_{\alpha, \theta}^{\pi^0}$ (and sample from it), i.e. initialise with $\Lambda = \{\pi^0\}$ and $v_{\pi^0} = 1$
- 2 **for** $k = 1, \dots, N$ **do**
- 3 **Propagation:** Evaluate (and sample from, if needed) $\nu_{k|0:k-1}$ using Algorithm 3
- 4 **Update:** Evaluate (and sample from) $\nu_{k|0:k}$ using Algorithm 5

Algorithm 7: Smoother – Sampling $X(t_k)$ given $\pi^{0:N}$

Input: Partitions $\pi^{0:N}$; sample size M

- 1 Evaluate $\nu_{k|0:k}$ using Algorithm 6, i.e. compute $\{w_\lambda, \lambda \in \Lambda_{0:k}\}$
- 2 Evaluate $\nu_{k|k+1:N}$, i.e. propagate the result of Algorithm 6 with $\pi^N, \pi^{N-1}, \dots, \pi^{k+1}$ given as input in this order, i.e. compute $\{h_\omega, \omega \in \Omega^{k:N}\}$
- 3 $\text{coag}(\Lambda_{0:k}, \Omega^{k:N}) \leftarrow \emptyset$
- 4 **for** $\lambda \in \Lambda_{0:k}, \omega \in \Omega^{k:N}$ **do**
- 5 **for** $\mu \in \text{coag}(\lambda, \omega)$ **do**
- 6 $\text{coag}(\Lambda_{0:k}, \Omega^{k:N}) \leftarrow \text{coag}(\Lambda_{0:k}, \Omega^{k:N}) \cup \mu$
- 7 Initialization: $s_\mu \leftarrow 0$ if s_μ is NULL
- 8 $s_\mu \leftarrow s_\mu + \frac{v_\lambda}{\text{PSF}_{\alpha,\theta}(\lambda)} \frac{h_\omega}{\text{PSF}_{\alpha,\theta}(\omega)} \mathcal{H}(\lambda, \omega | \mu) \text{PSF}_{\alpha,\theta}(\mu)$
- 9 Normalize $\{s_\mu, \mu \in \text{coag}(\Lambda_{0:k}, \Omega^{k:N})\}$
- 10 Draw $\mu_m \sim s_\mu$ and $X_m \sim \text{PD}_{\alpha,\theta}^{\mu_m}$ using Algorithm 2, for $m = 1, \dots, M$
- 11 **return** $\{s_\mu, \mu \in \text{coag}(\Lambda_{0:k}, \Omega^{k:N})\}$ and $\{X_m, m = 1, \dots, M\}$

Algorithm 8: Sampling further partitions given $\pi^{0:N}$

Input: Partitions $\pi^{0:N}$; weights $\{w_\lambda, \lambda \in \Lambda\}$ from $\Pr_{\alpha,\theta}(X(t) \in dx | \pi^{0:N})$; partition size m

- 1 Draw $\lambda \sim w_\lambda$
- 2 Simulate the next m steps of the CRP started from λ , i.e. sample $\Pi_{1:|\lambda|+m} | \Pi_{1:|\lambda|} = \lambda$
- 3 **return** the partition $\Pi_{|\lambda|+1:|\lambda|+m}$ induced by the last m customers

A.5.2 Weights of filtering and smoothing distributions

We collect here additional details on the mixture weights for filtering and smoothing.

Filtering. Empirically, most probability mass concentrates on a small subset of mixture components, which supports pruning. Figure 11 illustrates the proportion of mixture components required to reach different cumulative thresholds. Simulation results (with $T = 19$, $\Delta_k = 0.1$, $\alpha = 0.1$, $\theta = 1.5$, partitions of size 10, and 10^5 Gillespie particles) show that pruning away the least-weighted components retains nearly all the mass. Cf. Figure 7 for a performance comparison of pruning strategies.

Smoothing. The smoothed law $\nu_{k|0:N}$ from Theorem 4 combines information from past data $\pi^{0:k}$ and future data $\pi^{k+1:N}$. For any measurable $A \subset \nabla$,

$$\nu_{k|0:N}(A) = \int_A \nu_{k|0:k}(dx) \Pr(\Pi^{k+1} = \pi^{k+1}, \dots, \Pi^N = \pi^N | X(t_k) = x),$$

(cf. (31)), which separates the forward contribution $\nu_{k|0:k}$ (Theorem 3) from the backward contribution (the cost-to-go likelihood) conditional on the state x .

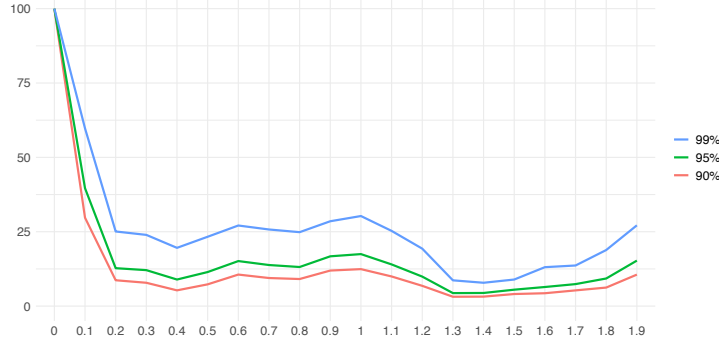


Figure 11: Proportion of filtering mixture components needed to reach 90%, 95%, and 99% cumulative probability.

In practice, evaluating $\text{Coag}_{\alpha,\theta}(\lambda, \omega)$ and its probabilities is most convenient via Proposition 5, using

$$\Pr(\Pi_{1:|\lambda|} = \lambda, \Pi_{|\lambda|+1:|\lambda|+|\omega|} = \omega) = \sum_{\mu \in \text{coag}(\lambda, \omega)} \mathcal{H}(\lambda, \omega \mid \mu) \text{PSF}_{\alpha,\theta}(\mu),$$

and

$$\Pr(\Pi_{1:|\lambda|+|\omega|} = \mu \mid \Pi_{1:|\lambda|} = \lambda, \Pi_{|\lambda|+1:|\lambda|+|\omega|} = \omega) = \frac{\mathcal{H}(\lambda, \omega \mid \mu) \text{PSF}_{\alpha,\theta}(\mu)}{\sum_{\mu' \in \text{coag}(\lambda, \omega)} \mathcal{H}(\lambda, \omega \mid \mu') \text{PSF}_{\alpha,\theta}(\mu')}.$$

Consequently, the smoothing weights can be computed in the equivalent, implementation-friendly form

$$s_\mu(\Delta_{k+1}) \propto \sum_{\lambda \in \Lambda_{0:k}} \sum_{\omega \in \Omega^{k:N}} \frac{v_\lambda}{\text{PSF}_{\alpha,\theta}(\lambda)} \frac{h_\omega(\Delta_{k+1})}{\text{PSF}_{\alpha,\theta}(\omega)} \mathcal{H}(\lambda, \omega \mid \mu) \text{PSF}_{\alpha,\theta}(\mu),$$

which is what Algorithm 7 evaluates.

A.5.3 Further figures

Figure 12 displays filtering (left column) and smoothing (right column) estimates of the three largest system coordinates (top to bottom), as described in Sections A.4.1 and A.4.2. The plotted data (diamonds) are the observed relative frequencies at the corresponding ranks. For example, the second panel shows the relative frequency of the second-largest group. Although presented separately for visualization, these estimates are obtained jointly for the full ∇ -valued vector, and the data are likewise used jointly to condition the model.

In Section 4.5 of the main text we noted that the bootstrap particle filter (BPF) can produce multimodal posterior densities, which is undesirable. This occurs, for instance, at the fifth observation time. Figure 13 provides a magnified comparison of the marginal posterior densities at that time, contrasting the BPF with the duality-based filter for two kernel bandwidths (0.001 and 0.01).

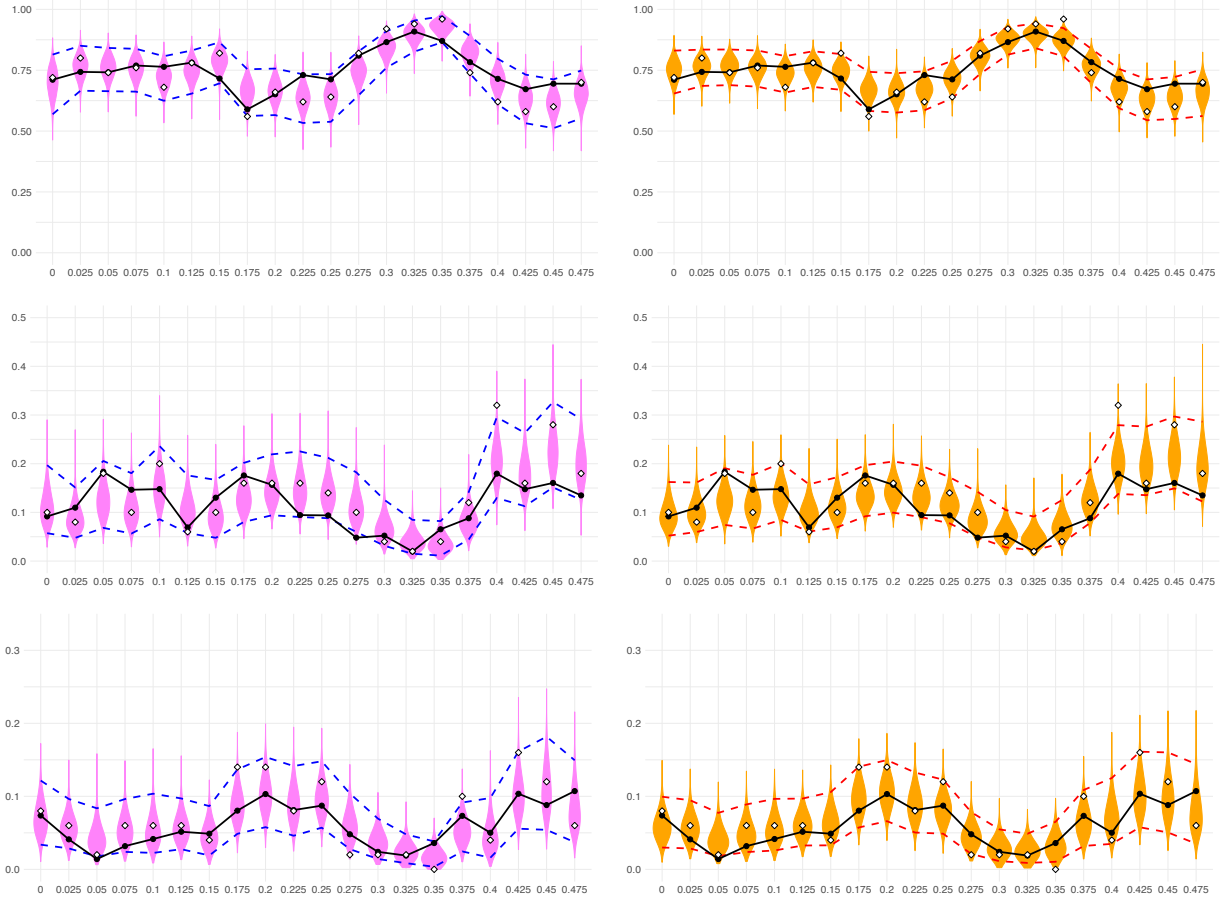


Figure 12: Filtering (left) and smoothing (right) posterior estimates for the three largest coordinates of the system. Violin plots with dashed intervals show posterior distributions and 95% credible intervals; solid black lines denote the true values; diamonds indicate observed relative frequencies.

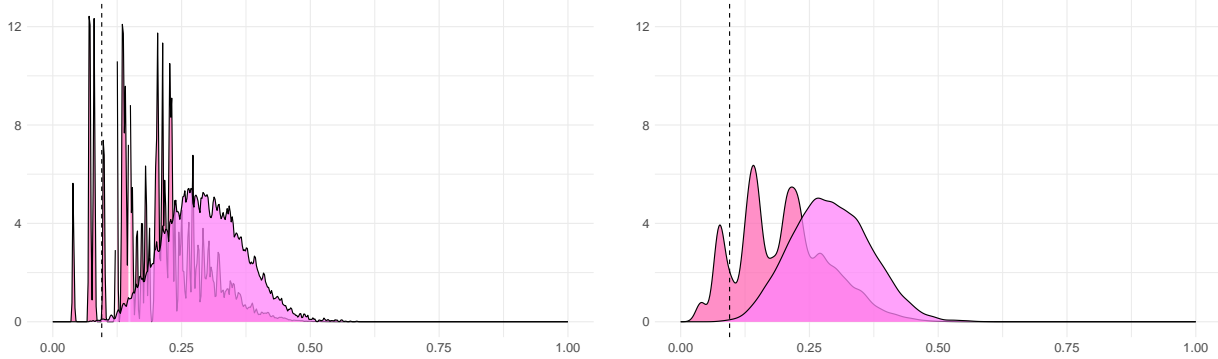


Figure 13: Marginal filtering densities at the fifth observation time, comparing the bootstrap particle filter (pink) with the dual filter (blue) under two kernel bandwidths (left: 0.001; right: 0.01). The vertical dashed line marks the observed heterozygosity.

Despite identical bandwidths, the dual filter yields smoother posteriors. While the multimodality under the BPF could be mitigated by increasing the number of particles, this is computationally prohibitive in practice.

References

Ascolani, F., Lijoi, A., and Ruggiero, M. (2023). Smoothing distributions for conditional Fleming–Viot and Dawson–Watanabe diffusions. *Bernoulli*, 29(2):1410–1434.

Balocchi, C., Favaro, S., and Naulet, Z. (2022). Bayesian nonparametric inference for “species-sampling” problems. *arXiv preprint arXiv:2203.06076*.

Baum, L. E. and Petrie, T. (1966). Statistical inference for probabilistic functions of finite state Markov chains. *The annals of mathematical statistics*, 37(6):1554–1563.

Beal, M., Ghahramani, Z., and Rasmussen, C. (2001). The infinite hidden Markov model. *Advances in neural information processing systems*, 14.

Bunge, J. and Fitzpatrick, M. (1993). Estimating the number of species: a review. *Journal of the American Statistical Association*, 88(421):364–373.

Cappé, O., Moulines, E., and Rydén, T. (2005). *Inference in Hidden Markov Models*. Springer series in statistics.

Caron, F., Neiswanger, W., Wood, F., Doucet, A., and Davy, M. (2017). Generalized Polya Urn for Time-Varying Pitman-Yor Processes. *Journal of Machine Learning Research*, 18(27):1–32.

Cereda, G., Corradi, F., and Viscardi, C. (2023). Learning the two parameters of the poisson–dirichlet distribution with a forensic application. *Scandinavian Journal of Statistics*, 50(1):120–141.

Chaleyat-Maurel, M. and Genon-Catalot, V. (2006). Computable infinite-dimensional filters with applications to discretized diffusion processes. *Stochastic processes and their applications*, 116(10):1447–1467.

Chaleyat-Maurel, M. and Genon-Catalot, V. (2009). Filtering the Wright-Fisher diffusion. *ESAIM: Probability and Statistics*, 13:197–217.

Chatzis, S. P. and Tsechpenakis, G. (2010). The infinite hidden Markov random field model. *IEEE Transactions on Neural Networks*, 21(6):1004–1014.

Chopin, N. and Papaspiliopoulos, O. (2020). *An introduction to sequential Monte Carlo*, volume 4. Springer.

Costantini, C., De Blasi, P., Ethier, S. N., Ruggiero, M., and Spano, D. (2017). Wright–Fisher construction of the two-parameter Poisson–Dirichlet diffusion. *The Annals of Applied Probability*, pages 1923–1950.

Ethier, S. N. (2014). A property of Petrov’s diffusion. *Electron. Commun. Probab.*, 19:1–4.

Feng, S. (2010). *The Poisson-Dirichlet distribution and related topics: models and asymptotic behaviors*. Springer Science & Business Media.

Feng, S. and Sun, W. (2010). Some diffusion processes associated with two parameter Poisson–Dirichlet distribution and Dirichlet process. *Probability theory and related fields*, 148(3):501–525.

Feng, S., Sun, W., Wang, F.-Y., and Xu, F. (2011). Functional inequalities for the two-parameter extension of the infinitely-many-neutral-alleles diffusion. *Journal of functional analysis*, 260(2):399–413.

Gael, J., Teh, Y., and Ghahramani, Z. (2008). The infinite factorial hidden Markov model. *Advances in Neural Information Processing Systems*, 21.

Gillespie, D. T. (2007). Stochastic simulation of chemical kinetics. *Annu. Rev. Phys. Chem.*, 58(1):35–55.

Gneiting, T. and Raftery, A. E. (2007). Strictly proper scoring rules, prediction, and estimation. *Journal of the American statistical Association*, 102(477):359–378.

Griffiths, R. C. (1984). Asymptotic line-of-descent distributions. *Journal of Mathematical Biology*, 21:67–75.

Griffiths, R. C., Ruggiero, M., Spano, D., and Zhou, Y. (2024). Dual process in the two-parameter Poisson–Dirichlet diffusion. *Stochastic Processes and their Applications*, 104500.

Holmes, I., Harris, K., and Quince, C. (2012). Dirichlet multinomial mixtures: generative models for microbial metagenomics. *PLoS ONE*, 7(2):e30126.

Isella, L., Stehlé, J., Barrat, A., Cattuto, C., Pinton, J.-F., and Van den Broeck, W. (2011). What's in a crowd? Analysis of face-to-face behavioral networks. *Journal of theoretical biology*, 271(1):166–180.

Jansen, S. and Kurt, N. (2014). On the notion (s) of duality for markov processes. *Probability Surveys*, 11:59–120.

Kalman, R. E. (1960). A New Approach to Linear Filtering and Prediction Problems. *Transactions of the ASME–Journal of Basic Engineering*, 82(Series D):35–45.

Kingman, J. F. C. (1978). The representation of partition structures. *Journal of the London Mathematical Society*, 2(2):374–380. Publisher: Oxford University Press.

Kon Kam King, G., Pandolfi, A., Piretto, M., and Ruggiero, M. (2024). Approximate filtering via discrete dual processes. *Stochastic Processes and their Applications*, 168:104268.

Kon Kam King, G., Papaspiliopoulos, O., and Ruggiero, M. (2021). Exact inference for a class of hidden markov models on general state spaces. *Electronic Journal of Statistics*, 15:2832–2875.

Papaspiliopoulos, O. and Ruggiero, M. (2014). Optimal filtering and the dual process. *Bernoulli*, 20(4):1999–2019.

Papaspiliopoulos, O., Ruggiero, M., and Spano, D. (2016). Conjugacy properties of time-evolving Dirichlet and gamma random measures. *Electronic Journal of Statistics*, 10:3452–3489.

Patil, G. and Taillie, C. (1982). Diversity as a concept and its measurement. *Journal of the American statistical Association*, 77(379):548–561.

Petrov, L. A. (2009). Two-parameter family of infinite-dimensional diffusions on the Kingman simplex. *Functional Analysis and its applications*, 43:279–296. Publisher: Springer.

Pitman, J. (1995). Exchangeable and partially exchangeable random partitions. *Probability theory and related fields*, 102(2):145–158.

Pitman, J. (2006). *Combinatorial stochastic processes: Ecole d'été de probabilités de saint-flour xxxii-2002*. Springer.

Pritchard, J. K., Stephens, M., and Donnelly, P. (2000). Inference of population structure using multilocus genotype data. *Genetics*, 155(2):945–959.

Tavaré, S. (1984). Line-of-descent and genealogical processes, and their applications in population genetics models. *Theoretical population biology*, 26(2):119–164.

Walker, S. G. and Ruggiero, M. (2009). Countable representation for infinite-dimensional diffusions derived from the two parameter Poisson–Dirichlet process. *Electronic Communications in Probability*, 14:501–517.

Wonham, W. M. (1965). Some Applications of Stochastic Differential Equations to Optimal Non-linear Filtering. *SIAM Journal on Control*, 2(3):347–369.